Coordination Chemistry Reviews 544 (2025) 216971

Contents lists available at ScienceDirect

Coordination Chemistry Reviews

journal homepage: www.elsevier.com/locate/ccr

Advances in metal-organic frameworks for cardiovascular therapy: from structural design to preclinical applications

Xueying Ge [a], Yongbin Liu [b], Xin Zhao [c], Ayman Nafady [d], Gogol Bhattacharya [a], Junhua Mai [b], Abdullah M. Al-Enizi [d], Roderic I. Pettigrew [a,*], Shengqian Ma [e,*]

[a] School of Engineering Medicine/ENMED, Texas A&M University and Houston Methodist Hospital, Houston, TX 77030, USA
[b] Department of Nanomedicine, Houston Methodist Academic Institute, Houston, TX 77030, USA
[c] J. Mike Walker '66 Department of Mechanical Engineering, Texas A&M University, College Station, TX 77843, USA
[d] Department of Chemistry, College of Science, King Saud University, P.O. Box 2455, Riyadh 11451, Saudi Arabia
[e] Department of Chemistry, University of North Texas, 1508 W Mulberry St, Denton, TX 76201, USA

ARTICLE INFO

Keywords:
Metal-organic frameworks (MOFs)
Cardiovascular disease (CVD) treatment
Drug delivery
Atherosclerosis
Myocardial infarction
Critical limb ischemia
Nanoparticles

ABSTRACT

Cardiovascular diseases are projected to account for over 40 % of global mortality by 2030, with current pharmaceutical treatments limited by poor pharmacokinetics, suboptimal biocompatibility, and concerns regarding long-term safety. Nanoparticles, including organic soft and inorganic hard nanoparticles, have shown promise as drug delivery systems, but face challenges to sufficient loading capacity and surface functionalization. Metal-organic frameworks (MOFs), an emerging class of inorganic-organic hybrid porous coordination solids, have emerged as transformative materials in modern engineering medicine, overcoming these limitations due to their high specific surface areas, tunable porosity, and flexibility in design. These properties, which can be tailored by selecting appropriate organic linkers and metal-containing nodes, enable MOFs to excel in drug loading and targeted delivery while maintaining favorable biocompatibility, thereby offering significant potential in cardiovascular treatment. Despite being cataloged in over 90,000 structures, the translation of MOFs from basic research to preclinical evaluation and eventual clinical applications remains underexplored. This review aims to bridge this gap by focusing on the design of MOFs tailored for cardiovascular therapeutic applications. It discusses the structure and properties of MOFs, including their metal and ligand selection, cargo loading and encapsulation capabilities, functionalization strategies and carbonization techniques, while highlighting their potential in the treatment of cardiovascular diseases such as atherosclerosis, thrombosis, myocardial infarction, and critical limb ischemia. We also discuss the challenges and limitations associated with MOFs, including structural validation, reproducibility, scalability and toxicity concerns, along with their translational potential. By connecting the fundamental design principles of MOFs to their preclinical cardiovascular applications, this review aims to inspire further research into the translation of MOFs into effective treatment for cardiovascular disease.

1. Introduction

Cardiovascular diseases (CVDs) remain the leading cause of morbidity and mortality worldwide and are projected to account for over 40 % of global deaths by 2030 [1]. CVD encompasses a broad spectrum of conditions affecting the heart and blood vessels. A primary contributing factor is the accumulation of lipid-rich atherosclerotic plaques within arterial walls, which impairs blood flow and significantly increases the risk of acute ischemic events [2]. If left untreated, this progression can lead to complications such as myocardial infarction and critical limb ischemia [3]. These conditions are chronic in nature and often require long-term management to control symptoms, prevent progression, and reduce the risk of life-threatening complications. Despite advancements in cardiovascular treatments, the current pharmaceutical interventions face significant challenges, such as rapid clearance from circulation, poor tissue penetration, and off-target toxicity. This negatively affects treatment compliance, reduces drug efficacy, and increases side effects. Nanoparticles have emerged as a

This article is part of a Special issue entitled: 'MOF2024 Invited Only' published in Coordination Chemistry Reviews.

* Corresponding authors.
E-mail addresses: pettigrew@tamu.edu (R.I. Pettigrew), Shengqian.Ma@unt.edu (S. Ma).

https://doi.org/10.1016/j.ccr.2025.216971
Received 30 April 2025; Received in revised form 25 June 2025; Accepted 7 July 2025
Available online 21 July 2025

promising approach for overcoming these challenges in cardiovascular treatment, due to their nanoscale size, tunable physicochemical properties, and ability to integrate therapeutic agents, enabling controlled release and enhancing targeted delivery [4]. Currently, nanoparticle delivery systems used for cardiovascular treatment [5] can be broadly categorized into organic soft nanoparticles, such as polymer- and lipid-based nanoparticles [6], and hard inorganic nanoparticles, including silica, carbon-based nanoparticles, and metallic nanoparticles [7].

A novel category of drug delivery carriers, hybrid porous coordination solids known as metal-organic frameworks (MOFs), built from a combination of inorganic and organic components, has emerged as a transformative class of materials in modern engineering medicine [8]. MOFs, constructed from inorganic metal-containing nodes connected by multitopic organic linkers [9,10], offer exceptional design flexibility through precise tuning of these two components [11,12]. MOFs, due to their functional pore walls, well-defined porosity, high specific surface areas, and multiple coordination sites, offer extensive opportunities for functionalization, efficient loading and site-specific delivery of both hydrophobic and hydrophilic drugs via host-guest interactions [13–16]. Over the course of their development, MOFs have demonstrated broad therapeutic potential across various biomedical applications, including cancer treatment [17], immunotherapy [18], gene therapy [19], and the management of metabolic and CVDs [20]. The historical timeline highlights significant milestones, starting from early developments in drug delivery and imaging (MIL-series MOFs, 2010) [21], progressing through clinical trials for cancer therapies (2018) [22], advances in gene editing [23] and targeted gene silencing (2020) [24], and recent innovations in therapies for cardiovascular and metabolic disorders (2022−2023) [20]. Most recently, AI/ML-guided MOFs have been designed to enhance treatment strategies for pancreatic cancer (2025) [25].(Fig. 1) This progression underscores the versatility, adaptability, and increasing promise of MOFs across diverse therapeutic areas. These attributes underscore MOFs' potential for advancing cardiovascular treatments. While MOFs are gaining increasing attention in cardiovascular research, a significant gap remains in translating them from basic research to clinical applications. Despite over 90,000 MOF structures being cataloged [26], most research remains at the stage of structural design. The assessment of the translational potential of MOFs via rigorous evaluation of their biocompatibility, toxicity, and stability in biological fluids is still pending [27]. Bridging this gap is crucial for realizing the full potential of MOFs in preclinical cardiovascular nanomedicine.

This review aims to bridge the gap between fundamental MOF properties and their practical use in cardiovascular treatment, emphasizing the need for MOF design tailored to the demands of preclinical and translational medicine. Previous reviews have highlighted MOF applications in cardiovascular biomarker detection [41,42] (e.g., Troponin I, Cardiac Troponin T, C-reactive Protein, Creatine Kinase-MB and others), and MOFs as drug loading carriers [43–45], nanozymes [46], host matrices for nanocomposites [11], and MOF functionalized with polymers [47] and cell membranes [48]. This review focuses on summarizing MOF structures and their corresponding properties tailored for preclinical cardiovascular studies to advance future cardiovascular therapies. This review will first introduce the properties of MOFs, including their metal and ligand selection, cargo loading and encapsulation capabilities, functionalization strategies and carbonization techniques. Subsequently, it will follow to discuss the application of MOFs in preclinical cardiovascular treatment, such as atherosclerosis, thrombosis, myocardial infarction, critical limb ischemia, and vascular implants. The overall aim of this review is to provide a clear framework to inspire researchers to consider the fundamental design of MOF structures with a clear path toward preclinical validation and eventual clinical application in cardiovascular treatment.

2. The emergence of MOFs as a novel nanomedicine for CVDs

MOFs leverage the complementary benefits of soft organic systems, which enable good biocompatibility and clearance, and hard inorganic systems, which offer high loading capacity. This unique combination makes MOFs well suited for biomedical applications, particularly in cardiovascular treatment [16]. To highlight these differences, Table 1 compares drug-loading efficiencies, common surface-functionalization approaches, and clinical potential across three major nanoparticle categories: MOFs, organic soft nanoparticles, and inorganic hard nanoparticles.

The advantages of MOF in cardiovascular therapy can be summarized from the perspective of its structure and composition. First, MOF ligands and metal nodes can be strategically selected to impart therapeutic and integrated diagnostic functions. For example, metal nodes including Fe, Zn, and Cu can serve as catalytic centers for reactive species elimination, mimicking superoxide dismutase (SOD) activity, allowing MOFs to act as nanozymes for scavenging reactive oxygen species (ROS), which play a critical role in oxidative stress-related CVDs. Certain organic ligands, such as porphyrins, also exhibit intrinsic

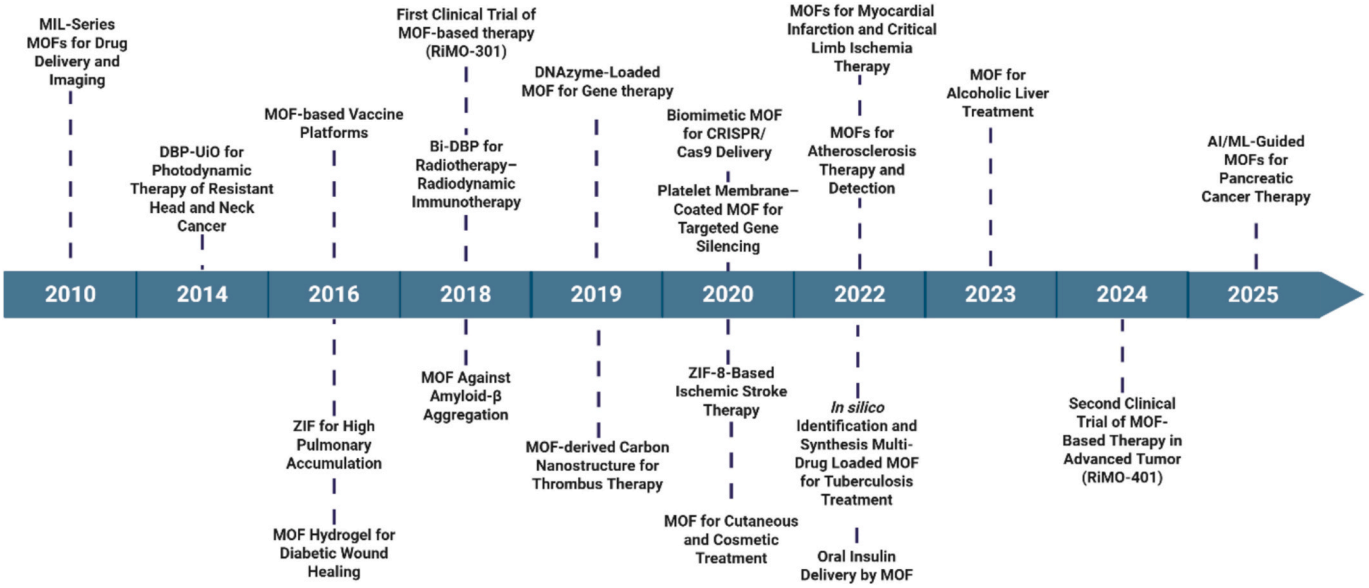

Fig. 1. A brief historical timeline highlighting key milestones in MOF-based therapeutic applications [17–21,23–25,28–40].

Table 1
Comparison of drug-loading efficiencies, surface functionalization methods, and clinical potential across nanoparticle types.

Different types of nanoparticles		Drug-loading efficiency	Functionalization method for targeting		Clinical nanoparticle therapeutics	reference
MOFs		Can reach up to 90 %, but depends on pore size and drug size	Non-covalent	Positively charged MOFs can absorb negatively charged peptides or DNA aptamers via electrostatic attraction.	RiMO-401and RiMO-301	[49]
			Covalent	Pendant ligand groups (e.g., amine (–NH_2), hydroxyl (–OH)) can be chemically modified to attach functional molecules without changing the MOF backbone.		
			Coordination	Functional molecules can coordinate to unsaturated metal sites in the MOF framework, or to metal-binding groups on the organic ligands (e.g., -OH or carboxyl (-COOH)) not involved in maintaining the framework structure.		
Organic soft nanoparticles	liposomes	Active loading (using internal pH gradient): >95 % Passive loading (during formation): ~30 %	Non-covalent	Cationic lipids provide a positive charge to the liposome surface, enabling negatively charged aptamers to bind via electrostatic attraction; Targeting moieties are given a hydrophobic "tail" (e.g., cholesterol) that embeds into the lipid bilayer, anchoring the ligand at the surface without disturbing the liposome.	FDA-approved liposomal products: Doxil® (marketed as Caelyx® in the EU/Canada), DaunoXome®, AmBisome®, DepoCyt®, Visudyne®, DepoDur® (withdrawn), Exparel®, Marqibo®, Onivyde®, Vyxeos®, Shingrix®, Arikayce®. Not FDA-approved in the U.S.: Myocet®, Mepact®, Lipusu®.	[50–55]
			Covalent	Ligands are chemically bonded to lipid headgroups using chemical reactions such as imide, amide, disulfide, thiol–maleimide, hydrazone, or click reactions.		
	Polymetric nanoparticles	Solvent evaporation/extraction: 6–100 % Interfacial deposition: >90 % Nanoprecipitation/solvent displacement: 33–77 % Emulsion-based methods: 48–87 % Double-emulsion/emulsification solvent-evaporation: 20–31 %	Non-covalent Covalent	Drugs or targeting ligands can be coupled via van der Waals, hydrogen bonding, or electrostatic interactions. Functionalization includes linker-mediated coupling (e.g., with PEG or silica), direct attachment through reactive groups (–NH_2, –COOH, –OH, thiol (–SH)), or plasma-based covalent treatment.	Clinically used platforms include polymeric micelles (Genexol®-PM, NK105, SP1049C, NC-6004, Nanoxel®, Apealea®), polymer–drug conjugates (Opaxio®, CRLX101), and targeted nanoparticles (BIND-014, CALAA-01).	[56,57]
Inorganic hard nanoparticles	Silica nanoparticles	Mesoporous silica nanoparticles: ~60 % Hollow silica nanoparticles: >90 %	Non-covalent	Adsorption via van der Waals, hydrogen bonding, or electrostatic interactions (e.g., poly(ethyleneimine), chitosan, poly-L-lysine adsorbed onto negatively charged ≡Si–O^-)	AuroShell® nanoparticles, Cornell Dots (C-dots, such as 124I-cRGDY–PEG–Cy5.5–C dot and 89Zr–cRGDY–Cy5–C dot), mesoporous silica nanoparticles (MSNs), and, as pharmaceutical excipients, fumed silica products like Aerosil® 300, Aerosil® 380, and Syloid® 224.	[58–61]
			Covalent	Co-condensation (incorporating organoalkoxysilanes during sol–gel synthesis) enables homogeneous pore-wall functionalization; post-synthesis grafting (silylation) attaches trialkoxysilanes to ≡Si—OH groups under anhydrous conditions to modify external or internal surfaces.		
	Metal nanoparticles (e.g., Gold Nanoparticles)	Solid metal nanoparticles have limited drug-loading capacity unless they are engineered with hollow architectures or surface functionalization (e.g., drug conjugation or polymer grafting).	Non-covalent	Biomolecules can be directly adsorbed onto citrate-capped gold nanoparticles via electrostatic/van der Waals interactions.	Clinical trials include CYT-6091, c19-A3, EMX-001 (naNODENGUE), naNO-COVID, NU-0129, AuroShell, gold nanoshells, CNM-Au8®.	[62,63]
			Covalent	Gold–thiolate bonds can be formed by direct thiolate–probe coupling (e.g., DNA, peptides, antibodies), self-assembled monolayers of bifunctional thiolate linkers (HS–$(CH_2)_n$–X), ligand exchange on CTAB-stabilized nanorods, dual co-grafting, or enzymatic assembly via thiolate–DNA ligation.		

therapeutic activity, further enhancing ROS scavenging and anti-inflammatory effects. Additionally, metals such as Fe and Mn also serve as imaging agents in magnetic resonance imaging (MRI). High atomic number metals, such as Zr and Hf, can facilitate computed tomography (CT) imaging and contribute to radiotherapeutic strategies through ROS generation. Second, the high porosity and large channels of MOFs allow them to act as efficient therapeutic carriers, providing high cargo loading capacity, stable retention, and controlled release of bioactive agents. Third, the tunable framework of MOFs supports the encapsulation of larger molecules, including vulnerable biomacromolecules such as enzymes, proteins, and nucleic acids, preserving their biological activity and preventing their degradation. Fourth, multiple functionalities, such as targeting moieties and stimuli-responsive components [64], can be incorporated into MOFs through surface chemistry, either via covalent conjugation to the organic linker or coordinative functionalization at the metal sites, enabling active drug delivery and controlled drug release, where therapeutic payloads are selectively released in response to biological triggers such as pH changes, redox conditions, or enzymatic activity. Fifth, MOFs can serve as sacrificial templates for constructing mesoporous carbon or carbon-metal/metal oxide nanostructures with enhanced nanozyme properties (Fig. 2).

The following section summarizes five key structural and compositional factors essential for the rational design of MOF-based diagnostic and therapeutic strategies for CVD treatment: metal node selection and organic ligand choice, pore structure for cargo loading and

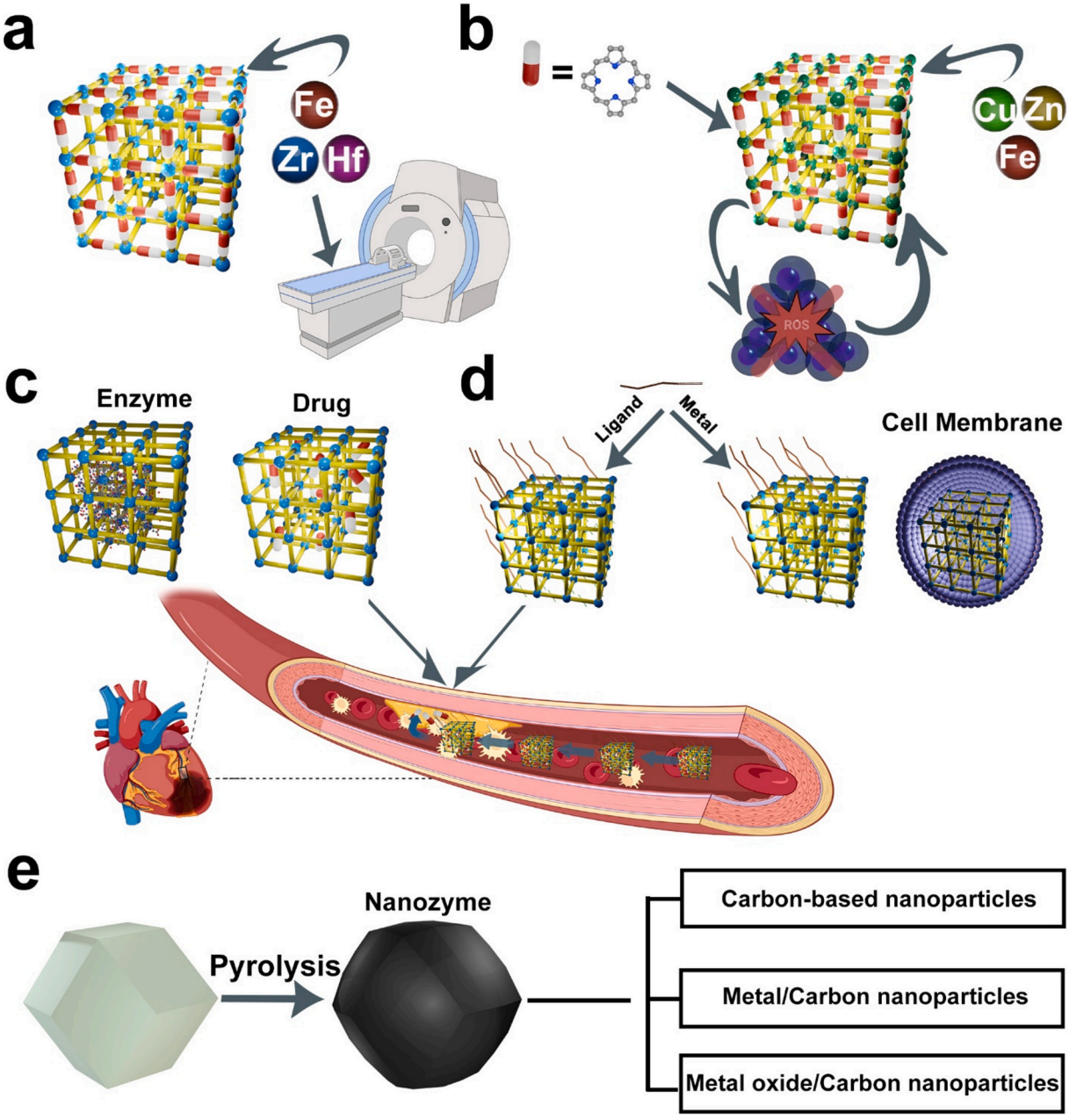

Fig. 2. (a) MOF metal nodes serving as contrast agents for MRI, CT, and as radiotracers for positron emission tomography (PET) imaging; (b) MOF metal nodes and ligands acting as therapeutic agents for ROS scavenging; (c) Enzyme and drug loading into MOF carriers; (d) Functionalization of MOFs through modifications at metal nodes and organic ligands, along with cell membrane coating on the MOF surface. The integration of drug loading and functionalization within the MOF structure facilitates targeted drug delivery. (e) MOFs employed as sacrificial templates for the synthesis of carbon-based materials and metal or metal oxide/carbon nanocomposites.

encapsulation, functionalization potential, and carbonization capability, providing insights for research design and MOF selection in cardiovascular applications. By combining these structural features, multifunctional platforms can be developed to enhance therapeutic efficacy. For example, a recent Phase I clinical trial involved an Hf-based MOF with a porphyrin ligand for radiodynamic therapy and radiotherapy, serving as an exemplary multifunctional MOF platform. The Hf metal nodes, due to their heavy atomic weight, are capable of absorbing X-ray photons, which are then transferred to the porphyrin photosensitizer, generating ROS for tumor cell destruction [18,65]. This example highlights the potential of MOFs as multifunctional therapeutic agents, a concept that can be readily extended to cardiovascular treatment by leveraging similar design strategies, particularly through tailored ligand and metal node functionalization.

2.1. Metal-containing nodes in MOFs

The metal-containing nodes in MOFs can play a pivotal role in the treatment of CVDs, as metals are involved in essential biological processes such as enzyme activation, inflammatory responses, cellular behavior, and protein synthesis [66]. In addition to their direct therapeutic effects, certain metal nodes can endow MOFs with imaging capabilities that support real-time disease monitoring and treatment planning. For example, paramagnetic metal-based MOFs, such as those containing Fe, Gd, and Mn, have been used as MRI contrast agents for non-invasive assessment of cardiac function and vascular abnormalities [67,68]. Alternatively, MOFs constructed with heavy metal atoms, such as Hf and Zr (e.g., UiO-66) enhance X-ray absorption for radiodynamic and radiotherapeutic therapies, as well as for CT imaging with high spatial and contrast resolution [16,67,69]. MOFs incorporating isotopes such as ^{89}Zr (e.g., UiO-66) and ^{64}Cu (e.g., PCN-222) allow for PET imaging [70], enabling dynamic imaging of biological changes at the cellular and subcellular dimensions during the early stages of heart disease [71], thereby informing future therapeutic strategies. These imaging-guided functions not only facilitate early diagnosis but also enable real-time evaluation of therapeutic responses, positioning MOFs as promising theranostic platforms for CVDs. The structural tunability of MOFs further allows for the integration of both therapeutic and diagnostic functionalities within a single platform, advancing the precision and efficacy of cardiovascular treatments [72].

Beyond their role in diagnostic imaging, MOFs can be rationally designed with specific metal nodes to enable diverse therapeutic applications. For example, MOFs containing metals such as Fe, Cu, Mn, and Co exhibit catalase (CAT)-mimicking activity, while those with Zn, Cu, Mn, or Fe can mimic SOD activity [73]. Compared to natural enzymes, these nanozyme-like MOFs offer higher stability and lower cost, making them attractive for biomedical use [74]. Acting as nanozymes, they demonstrate antioxidant capabilities by scavenging ROS, which is particularly relevant for CVD treatment. Excessive ROS critically influences inflammation, irregular shear stress from disturbed blood flow, and vascular wall remodeling. In conditions such as thrombosis and myocardial infarction, elevated ROS levels can accelerate tissue damage, leading to worse clinical outcomes [75]. Therefore, these MOF-based nanozymes have great potential in managing CVDs by reducing oxidative stress, supporting tissue repair, and preventing complications such as endothelial dysfunction and thrombosis. Furthermore, MOF-based nanozymes exhibit higher catalytic potency than natural enzymes due to the tunable cavities and channels within MOF structures. These features not only mimic the hydrophobic coordination environments found in natural enzymes but also function as microreactors, thereby improving catalytic efficiency. The porous structure of MOFs facilitates the optimal utilization of atoms for enzyme-like catalysis, further improving their therapeutic potential [76,77].

Beyond their nanozyme properties, Zn- and Cu-based MOFs have shown significant potential in promoting vascular endothelial cell morphogenesis and treating ischemic diseases. Zn is an essential nutrient and a key regulator of vascular health and disease, playing a crucial role in endothelial cell function by modulating angiogenesis, inflammation, and blood clotting [78]. Similarly, Cu is vital for angiogenesis and vasculogenesis, as it stimulates endothelial cell migration and enhances the expression of key angiogenic growth factors. Specifically, Cu enhances the stability of hypoxia-inducible factor 1α (HIF-1α) by suppressing factor-inhibiting hypoxia-inducible factor 1 (FIH-1) activity, leading to increased expression of pro-angiogenic growth factors such as vascular endothelial growth factor (VEGF). This promotes endothelial cell proliferation, migration, and neovascularization, supporting tissue regeneration and blood flow recovery in ischemic conditions [79]. However, excessive free Zn^{2+} and Cu^{2+} ions can lead to heightened ROS production and cytotoxicity [80], which can be mitigated by Zn- and Cu-based MOFs, as they enable controlled release of Zn^{2+} and Cu^{2+} ions through gradual disassembly of the MOF structure under acidic conditions. This approach ensures that metal ions remain at therapeutically effective levels while minimizing the risks associated with excessive metal ion exposure. Zn-based MOFs, such as those from the ZIF series, have demonstrated the ability to improve cardiac function and reduce myocardial damage caused by ischemia-reperfusion injury [81,82]. Likewise, Cu-based MOFs, such as HKUST-1, have been shown to stabilize HIF-1α for prolonged periods, thereby enhancing blood perfusion and promoting vascular repair [79].

Cu-based MOFs, such as HKUST-1, have also shown promise in catalyzing the decomposition of S-nitrosothiols (RSNOs) through a Cu-mediated catalytic pathway, facilitating the controlled release of nitric oxide (NO). The pores of HKUST-1 enhance the accessibility and diffusion of RSNOs, facilitating their interaction with the framework's unsaturated Cu metal sites [83]. NO is a crucial gasotransmitter that regulates cardiovascular function by promoting vasodilation and modulating blood pressure. However, endothelial dysfunction can reduce NO bioavailability, leading to various cardiovascular complications, including impaired endothelium-dependent vasodilation, thrombosis, vascular inflammation, and intimal proliferation [84]. To address impaired endogenous NO production, various Cu-based MOFs, such as MOF-199 and HKUST-1, have been used as coatings on stents and vascular graft materials. These MOF coatings catalyze RSNOs, facilitating NO release and improving vascular function in implant applications [85–87].

2.2. MOF ligands

The selection of biomolecular ligands, including proteins, nucleobases, polypeptides, amino acids, cyclodextrins, and porphyrins/metalloporphyrins, is crucial for constructing multifunctional MOFs with controlled drug release, biomimetic catalysis, and imaging capabilities, as well as for enhancing their biocompatibility. Among these ligands, porphyrin-based ligands, such as those in PCN-222 and PCN-224, stand out due to their versatile functionalities. Specifically, porphyrins serve as photosensitizers in photodynamic therapy (PDT) and as photoabsorbing agents for photothermal therapy (PTT) [44]. In PDT, porphyrin-based MOFs can act as photosensitizers to facilitate the generation of ROS under light activation [88], which exhibit thrombolytic properties [32], making them promising for the treatment of atherosclerosis and thrombosis. In addition to their role in ROS generation, porphyrin-based MOFs exhibit enzyme-mimicking properties, simulating the function of key antioxidant enzymes such as SOD and CAT to eliminate excess ROS. This ROS-scavenging capability is particularly beneficial in treating myocardial infarction, where oxidative damage and inflammation contribute to cardiac tissue damage [89]. Beyond their therapeutic potential, porphyrin-based MOFs possess intrinsic fluorescence, enabling non-invasive imaging and real-time biomarker detection in atherosclerosis diagnosis [38,90,91]. These combined properties highlight the potential of porphyrin-based MOFs as versatile platforms for both the treatment and monitoring of CVDs.

Cyclodextrin, when used as a ligand to construct MOFs, offers

excellent biocompatibility and low toxicity due to its unique structure, which features a hydrophobic cavity and a hydrophilic outer surface. This structural characteristic allows cyclodextrins to form inclusion complexes with guest molecules, making them highly suitable for the delivery of cardiovascular drugs [92]. Furthermore, the hydroxyl groups on cyclodextrin molecules can be readily modified to tailor drug release behavior and enhance the stability of drug delivery systems [93]. Cyclodextrin-based MOFs have been explored as drug carriers for targeted thrombolytic therapy by loading thrombolytic agents such as urokinase plasminogen activator (uPA) [94], and cardioprotective compounds like trans-sodium crocetinate [95].

2.3. Cargo loading and encapsulation in MOFs

The pore structure of MOFs can be utilized for loading drugs and therapeutic agents for CVD treatment. Due to the versatility of metal-containing nodes and organic ligands, the pore size of MOFs [96] can be adjusted to accommodate the specific requirements of different therapeutic agents. Additionally, MOFs possess hydrophilic metal-containing nodes and hydrophobic organic ligands, making them suitable for loading both hydrophilic and hydrophobic drugs, enhancing their applicability for a wide range of cardiovascular therapies [97].

Table 2 below summarizes the most commonly used MOFs in cardiovascular research, detailing their metal nodes and ligands, pore diameters estimated from pore size distribution analyses based on N_2 adsorption data at 77 K and Brunauer-Emmett-Teller (BET) surface areas. It is important to note that pore size distribution derived from N_2 adsorption provides an indirect estimation of the internal pore diameters and may not accurately represent the window sizes, which are critical for molecular diffusion and drug loading [16]. Nevertheless, this information helps researchers in selecting suitable MOFs based on drug size and loading capacity. Additionally, representative MOFs from the same structural families are also included to offer further insights into MOF carrier selection and design. This table serves as a reference for optimizing MOF applications in CVD treatment.

Some macromolecular therapeutic agents, such as enzymes, proteins, and RNA, are significantly larger than the pore windows of many MOFs, posing challenges for effective encapsulation. To address this problem, various techniques have been employed to incorporate these larger biomolecules within MOFs, including microfluidic techniques, the hard templating method, and the one-pot embedding method [141]. Microfluidic techniques, which are commonly used for synthesizing lipid nanoparticles [142] rely on continuous flow mixing of two solutions: an aqueous metal ion solution containing the target biomolecule, and an organic linker dissolved in an organic solvent. The mixing occurs within microchannels, enabling biomolecule encapsulation within MOFs [143]. The hard templating method utilizes calcium carbonate ($CaCO_3$) microparticles as a structural template, which is immersed in an MOF precursor solution to facilitate MOF growth around it. After removal of the $CaCO_3$ template, the resulting porous structure provides sufficient space for the encapsulation of large biomolecules [144]. The one-pot method, also known as biomimetic mineralization, is widely used for encapsulating enzymes [141], RNA [145,133] and other biomolecules within MOFs. In this approach, the biomolecule acts as a nucleation center, guiding the self-assembly of MOF precursors under physiological conditions. As the metal-organic coordination progresses, the MOF framework gradually forms around the biomolecules, forming a protective shell that not only enhances stability and preserves the biological activity of the encapsulated biomolecule but also shields it from degradation in lysosomes, thereby enhancing its bioactivity in therapeutic applications [146].

MOFs' cargo loading and encapsulation capabilities can be leveraged to embed guest species, such as metal and metal oxide nanoparticles, either within MOF pores or inside MOF structures using various strategies, including the 'ship-in-a-bottle' strategy, the 'bottle-around-ship' strategy, the 'layer-by-layer' strategy, and the 'one-pot' strategy [11,147,148]. For encapsulation within MOF pores, the pore windows must be compatible with the dimensions of the guest species to ensure proper loading. Alternatively, MOFs can act as host matrices, providing spatial confinement for nanoparticles due to their well-defined pore structures and coordination environments. This confinement prevents nanoparticle aggregation, thereby enhancing their intrinsic properties. As a result, MOF-nanoparticle composites can significantly enhance their functional properties and show exciting potential as multifunctional agents for cardiovascular treatment. For example, incorporating iron oxide nanoparticles into MOFs increases their magnetization, thereby improving relaxivity and enhancing their performance as both an MRI contrast agent and a magnetothermal therapy agent [103]. Similarly, embedding gold nanoparticles within MOFs grants peroxidase (POD) and CAT-mimicking activities, enabling catalytic decomposition

Table 2
MOF metal nodes, ligands, pore sizes and BET surface areas.

MOFs	Metal nodes	Ligands	Pore Diameter (nm)	BET surface areas ($m^2\ g^{-1}$)	Refs
HKUST-1	$Cu(NO_3)_2{\cdot}2.5H_2O$	benzene-1,3,5-tricarboxylic acid	~0.4	1486	[98]
MOF-199	$Cu(NO_3)_2{\cdot}3H_2O$	benzene-1,3,5-tricarboxylic acid	0.52	1459	[99]
UiO-66	$ZrCl_4$	Terephthalic acid	0.85 and 1.3	1580	[100]
UiO-67	$ZrCl_4$	biphenyl-4,4′-dicarboxylate	1.15 and 2.3	2500	
UiO-66(Hf)	$HfCl_4$	Terephthalic acid	0.6 and 0.8	655	[101,102]
UiO-66-NH_2	$ZrCl_4$	2-aminoterephthalic acid	0.7 and 1.5	1202	[103]
UiO-66(Ce)	$Ce(NH_4)_2(NO_3)_6$	Terephthalic acid	0.8 and 1.3	1282	[104,105]
MIL-88B[a]	$FeCl_3{\cdot}6H_2O$	Terephthalic acid	<0.38	8	[106]
MIL-53[a]	$FeCl_3{\cdot}6H_2O$	Terephthalic acid	0.6[b]	5	[107]
MIL-100	$FeCl_2$	benzene-1,3,5-tricarboxylic acid	1.84 and 2.23	2028	[108]
MIL-101	$FeCl_3{\cdot}6H_2O$	terephthalic acid	~1.2 and ~ 2.7	3124	[109]
MIL-101-NH_2	$FeCl_3{\cdot}H_2O$	2-aminoterephthalic acid	~1.5 and ~ 2.4	1652	[110]
ZIF-8	$Zn(NO_3)_2{\cdot}6H_2O$	2-methylimidazole	~1.0	1630	[111,112]
ZIF-90	$Zn(NO_3)_2{\cdot}4H_2O$	Imidazolate-2-carboxyaldehyde	1.87	897	[113,114]
PCN-222	$ZrCl_4$	H_2TCPP	~1.2 and 3.19	2223	[115]
PCN-222(Mn)	$ZrCl_4$	MnTCPPCl	~1.2 and 2.97	2046	
PCN-222(Fe)	$ZrCl_4$	FeTCPPCl	~1.3 and 3.2	2220	
PCN-222(Co)	$ZrCl_4$	CoTCPP	~1.3 and 3	1864	
PCN-222(Zn)	$ZrCl_4$+ $ZnCl_2$	H_2TCPP	~1.3 and 3	1906	
PCN-222(Cu)	$ZrCl_4$	CuTCPP	~1.2 and 3.1	2312	
PCN-224	$ZrCl_4$	H_2TCPP	1.9	2600	[116,117]
γ-cyclodextrin-MOF (CD-MOF)	K_2CO_3	γ-cyclodextrin	~1	1220	[118]

TCPP: 5,10, 15, 20-Tetrakis (4-carboxyphenyl)porphyrin.
[a] means breathing MOF.
[b] means pore size is determined based on CO_2 adsorption data at 273 K.

of hydrogen peroxide (H_2O_2), and introduces a localized surface plasmon resonance effect, which can enhance the nanocomposite's potential for PTT. Incorporating platinum nanoparticles [149] into MOFs further expands their therapeutic potential by providing SOD-, POD-, and CAT-like enzymatic activities, enabling enhanced antioxidative and catalytic effects. Additionally, encapsulating upconversion nanoparticles within MOFs enables the conversion of near-infrared (NIR) light into visible light, which can be leveraged for PDT [11]. Although few of these nanoparticle@MOF composites have been created and validated in vivo for CVD, we present them as a guide. By choosing the appropriate nanoparticles to incorporate, researchers can design MOF-based nanocomposites that combine multiple catalytic effects. For example, incorporating Se nanoparticles [150] into MOFs further endows the nanocomposites with glutathione peroxidase (GPx)-like activity and antisenescence properties, which may prevent the onset and progression of atherosclerosis [122].

2.4. Functionalization of MOFs

Functionalization of MOFs is essential to overcome their intrinsic instability and to preserve the structural integrity of the framework under physiological conditions. Introducing specific functional groups allows MOFs to be tailored for enhanced water dispersibility, reduced plasma protein binding, evasion of the reticuloendothelial system, and incorporation of affinity molecules for targeted drug delivery. These modifications improve the stability, performance, and precision of MOFs while reducing their toxicity in cardiovascular treatment [151]. MOF functionalization strategies primarily involve covalent and coordinate covalent modifications. Covalent modification involves the chemical alteration of pendant functional groups (e.g., amines, alcohols) on MOF ligands. These accessible groups, which do not contribute to the framework's backbone, act as reactive sites for attaching functional molecules. Coordinate covalent modification functionalizes the metal-containing nodes of MOFs without disrupting the framework topology. This modification can be achieved via two approaches: (1) binding to unsaturated metal sites, where external functional molecules coordinate to accessible metal-containing nodes in the MOF framework; and (2) metallation of organic ligands, where metal-binding groups (e.g., -OH or -COOH), which are present on the MOF ligands but not involved in maintaining the framework structure, coordinate with additional metal centers [152]. (Fig. 3a) When functionalizing MOFs with large molecular dimensions, steric hindrance must be considered. In such cases, functionalization is usually limited to the outer surface or the entrances of the pores to prevent clogging and ensure that the internal structure remains open for efficient drug loading and release [16].

Functionalizing MOFs with polymers enhances their biomedical performance by improving stability, biocompatibility, and targeting capabilities [47]. This enhancement is particularly important during systemic circulation, where phosphate ions, naturally present in the blood, may compete with organic linkers for coordination at metal sites of the MOF, potentially leading to MOF dissociation. Phosphate ions, as a hard base according to Pearson's hard and soft acids and bases theory [158], preferentially form stable coordination bonds with hard metals, which can interfere with the MOF structure. Therefore, polyethylene glycol (PEG) functionalization has emerged as a robust strategy. PEGylation not only stabilizes the MOF structure by shielding it from phosphate-induced degradation but also prevents premature drug release. Moreover, PEG chains on the MOF surface reduce recognition by the mononuclear phagocyte system and minimize protein adsorption during circulation, thereby enhancing circulation time and biocompatibility [159]. Recent approaches to PEGylating MOF surfaces primarily involve covalent modifications, such as using Cu-catalyzed azide-alkyne cycloaddition (CuAAC) (Fig. 3b) [153] to covalently attach PEG to the MOF ligand or employing radical-induced polymerization to covalently attach PEG on the MOF surface [154].(Fig. 3c) Additionally, phosphate-functionalized PEG can be incorporated into the MOF structure through coordination covalent binding with metal-containing nodes, leveraging the hard base properties of phosphate ions to form stable interactions with the metal sites [155] (Fig. 3d).

Beyond improving stability and circulation time, polymer functionalization also enables targeted delivery, enhancing the precision and efficacy of MOF-based cardiovascular therapies. For example, the functionalization of *dextran,* a naturally derived polysaccharide, facilitates macrophage targeting via receptor-mediated endocytosis. Key receptors involved in this process include the scavenger receptor A (SR-A), cluster of differentiation (CD)36, and the dextran receptor, which facilitate efficient internalization and cellular uptake, leading to the accumulation of dextran-functionalized MOFs in macrophage-rich regions, such as atherosclerotic plaques [160]. Several strategies have been developed to functionalize MOF surfaces with dextran. For example, phosphate-functionalized dextran can coordinate with metal sites in MIL-100 [157].(Fig. 3f) In another approach, spermine-modified acetalated dextran shells can be functionalized on the surface of ZIF-90 using a microfluidic method [156].(Fig. 3e) Additionally, dextran sulfate, when coated on PCN-222 through electrostatic adsorption, can target macrophages in atherosclerotic plaques by binding to SR-A, which is overexpressed on the surface of macrophages in these lesions. These strategies highlight the potential of dextran-coated MOFs as targeted therapeutic agents for cardiovascular treatment [68]. Alternatively, *hyaluronic acid (HA)*, a key component of the extracellular matrix, can also be leveraged for macrophage targeting, as HA selectively binds to the CD44 receptors, which are overexpressed on activated macrophages under inflammatory conditions such as atherosclerotic plaques. HA can be coordinately functionalized with the metal sites in the ZIF-8 framework through its carboxyl groups [161]. This functionalization enables HA-functionalized MOFs to effectively bind to CD44 receptors on macrophages, promoting receptor-mediated endocytosis and thereby enhancing the targeted delivery of MOFs to macrophage-rich regions [162].

Peptides are short sequences of amino acids, generally comprising fewer than 50 residues, and are frequently stabilized by disulfide bonds. They are rationally engineered to selectively bind to and influence specific protein-protein interactions [163]. In addition to being use as organic ligands to construct MOFs, peptides possess reactive terminal groups (–NH_2 and –COOH) that can be functionalized on MOFs by coordinating with metal sites or attaching to MOF ligands [164]. For example, a peptide dimer (Di-peptide(WQPDTAHHWATL)-PEG_{2000}-COOH) with a C-terminus was attached to the surface of ZIF-8 through charge interactions [165]. The F3 peptide (KDEPQRRSARLSAKPAPPK-PEPKPKKAPAKK), known for its selective binding to the activated endothelial cell surface, was conjugated to UiO-66 through a combination of thiol-maleimide reaction and surface charge interaction. First, a cysteine residue incorporated at the C-terminus of the F3 peptide reacted with the maleimide group on pyrene-PEG-maleimide via a thiol-maleimide reaction. The resulting functional molecular conjugate was then attached to the UiO-66 surface through surface charge interaction [70]. A breast tumor-targeting peptide was attached to polyethyleneimine [166], which was subsequently coated onto the surface of ZIF-8 through electrostatic interactions [167]. Moreover, peptide-targeting strategies have also shown promise in peripheral artery disease. For example, two peptides, an endothelial cell-targeting peptides and a mitochondria-localizing sequence peptides, were attached to ZIF-90 through a Schiff-base reaction, in which the N-terminus of the peptide reacts with an aldehyde group on ZIF-90. This peptide functionalization enabled ZIF-90 to target both vascular endothelial cells and mitochondria, thereby reducing the required dosage of Zn to stimulate mitochondrial production of ROS under ischemic conditions to activate the phosphoinositide 3-kinase (PI3K)/protein kinase B (Akt)/endothelial nitric oxide synthase (eNOS) pathway, promoting NO production, which supports endothelial cell growth, migration, and vascularization to treat ischemia in peripheral artery disease [36].

In addition to conventional coatings such as PEG, polymers, and

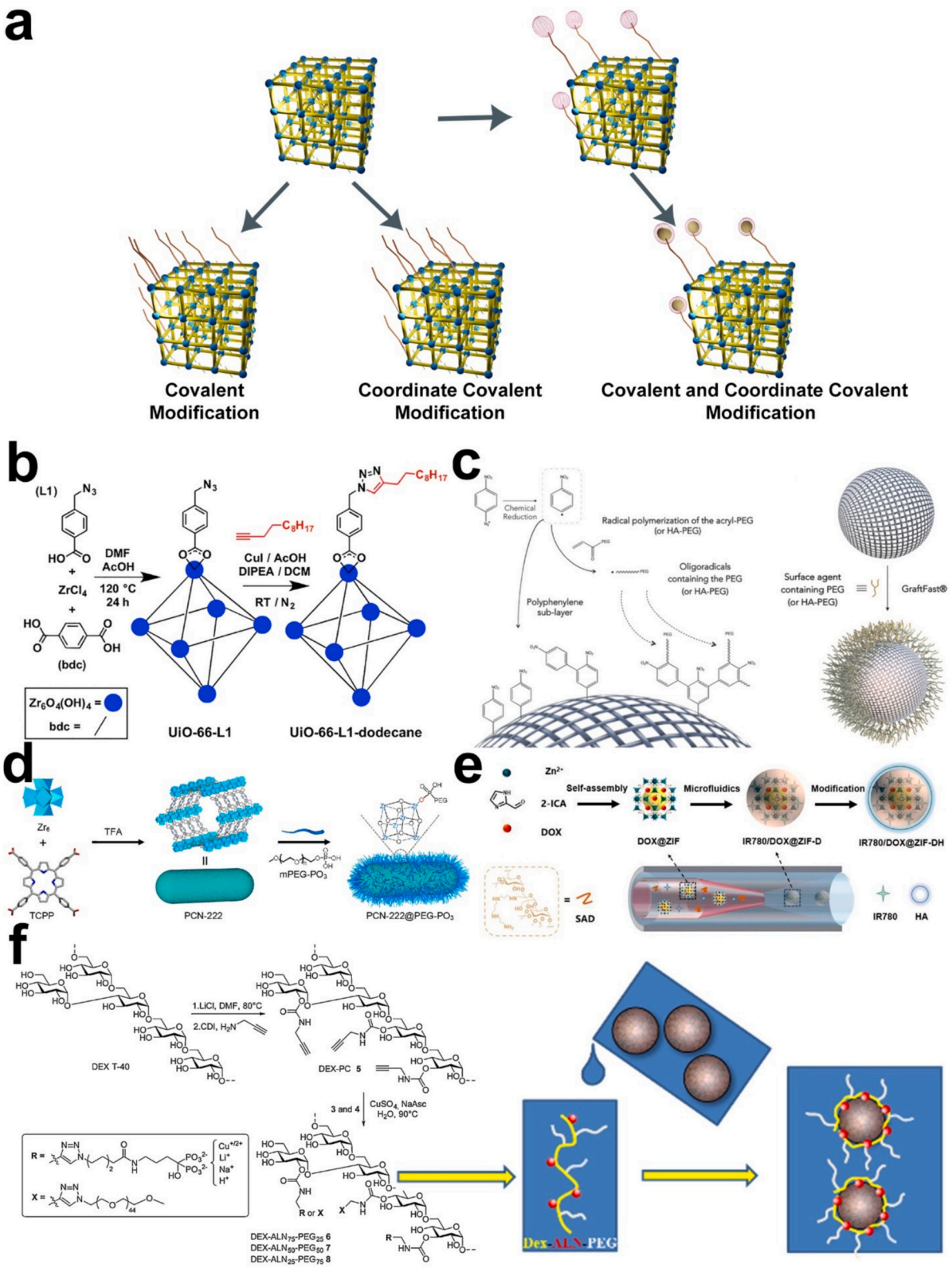

Fig. 3. (a) MOF functionalization strategies; (b) Surface modification of UiO-66 with alkanes; [153] Reproduced with permission. Copyright 2017, *Chem*. (c) Schematic of the GraftFast reaction and the preparation of MIL-100@PEG nanoparticles via GraftFast; [154] Reproduced with permission. Copyright 2018, *Small*. (d) Schematic of the postsynthetic modification of nanoMOFs with phosphate-functionalized methoxy polyethylene glycol (mPEG) groups. [155] Reproduced with permission. Copyright 2021, *J. Am. Chem. Soc*. (e) Schematic of a MOF coated with a spermine-modified acetalated dextran shell via a microfluidics-based self-assembly route. [156] Reproduced with permission. Copyright 2020, *ACS Appl. Mater. Interfaces*. (f) Schematic representation of the preparation of dextran-alendronate-PEG coated on nanoMOFs. [157] Reproduced with permission. Copyright 2023, *Carbohydr. Polym*.

peptides, cell membrane coating offers a biomimetic strategy to overcome nonspecific targeting and clearance limitations. These biomimetic MOF materials retain the physicochemical characteristics and biological functionalities of their source cells, enabling targeted delivery to diseased tissues while evading immune system recognition and clearance, ultimately prolonging circulation times through their natural camouflage. Cell membranes used to functionalize MOFs have been derived from a variety of sources, including blood-circulating cells such as red blood cells, platelets, neutrophils, macrophages and dendritic cells, as well as cancer cells and fused cells [48]. The cell membrane coating method for MOFs typically involves co-extrusion and ultrasonic techniques. The interaction between the cell membrane and the MOF is primarily charge-based, as MOFs have a positive charge due to the metal component, while cell membranes are negatively charged. Furthermore, terminal groups such as $–NH_2$ and –COOH can attach to the metal or ligands of the MOF structure, similar to the interaction between peptides and MOFs [168,169]. Recently, neutrophil membrane-coated MOFs have been utilized to treat atherosclerosis, leveraging the ability of neutrophil membranes to target inflamed endothelial cells at atherosclerotic sites via the interaction between the endothelial cell protein intercellular adhesion molecule 1 (ICAM-1) on endothelial cells and CD18 on the neutrophil-derived nanoparticle surface [123].

2.5. MOF-derived carbon materials

Mesoporous carbon materials derived from MOFs can be prepared using MOFs as sacrificial templates, offering enhanced stability through high-temperature pyrolysis. This process addresses the intrinsic instability of MOFs while retaining key advantages of their precursors, such as highly interconnected three-dimensional porosity and large surface area, thereby broadening their potential applications [77]. Upon carbonization, the metal centers within the MOF framework contribute to the functional enhancement of the resulting carbon materials [170]. This feature is particularly beneficial for the synthesis of heteroatom-doped carbon structures, such as single-atom catalysts featuring the widely applicable M-N-C site (where M represents a single metal atom). These single-atom nanomaterials can function as highly promising nanozymes due to their unsaturated coordination sites and distinctive electronic properties. Additionally, their controlled pore channels and cavity sizes facilitate the effective exposure of active sites, promote unobstructed diffusion pathways, and provide ample buffer space to accommodate structural changes during catalytic reactions [77,171]. These properties make them highly attractive for various applications, including cardiovascular medicine. MOF-derived nanoparticles have been extensively explored for thrombus therapy due to their multifunctional properties. For instance, mesoporous silica-coated ZIF-8-derived mesoporous carbon nanospheres containing porphyrin-like metal centers have demonstrated efficacy in PDT for thrombolysis [32]. MIL-101(Fe)-derived carbon nanoparticles, containing Fe elements from the MIL-101(Fe) precursor, have been investigated for magnetothermal and photothermal dual therapy in thrombus dissolution [127].

3. Applications for MOFs in CVD treatment

MOFs are gaining attention for treating CVDs due to their distinctive features, including high porosity, tunable structures, and multifunctionality. Their precise composition and surface control enable the development of tailored systems for specific therapeutic needs. Beyond serving as conventional drug carriers, the modular architecture of MOFs offers multifunctional capabilities by combining therapy, targeting, and diagnosis, which opens the door to integrated and personalized treatment for CVDs. This flexibility also allows for rational adaptation to diverse pathological environments, ranging from vascular repair to anti-inflammatory interventions. The following section will systematically summarize how the structural and compositional advantages of MOFs can be translated into functional outcomes across various preclinical CVD models, including atherosclerosis, thrombosis, myocardial infarction, critical limb ischemia, and vascular implants. By bridging the gap between materials science and the cardiovascular field, we will discuss each treatment approach, starting from the fundamental design principles and properties of MOFs to their evaluation in preclinical studies. The goal is to inspire researchers to integrate treatment mechanisms with intrinsic material design for more effective therapeutic strategies.

3.1. Atherosclerosis

Atherosclerosis is a chronic inflammatory condition primarily initiated by lipid accumulation and endothelial dysfunction. During the progression of atherosclerosis, foam cells, which secrete proinflammatory cytokines (e.g., tumor necrosis factor-alpha (TNF-α), interleukin-6 (IL-6), interleukin-1 beta (IL-1β))—mainly lipid-laden macrophages or vascular smooth muscle cells (VSMCs) that have engulfed oxidized low-density lipoprotein (oxLDL)—play a crucial role in the amplification of inflammation within the arterial walls and the formation of atherosclerotic plaques [172,173]. During disease progression, elevated ROS production significantly contributes to the proatherogenic processes in vasculature, resulting in lipid and DNA oxidation, endothelial dysfunction, and inflammation, all of which accelerate plaque progression [174]. Meanwhile, impaired autophagy in macrophages and foam cells disrupts cholesterol efflux, exacerbating lipid accumulation [175,176]. Additionally, the nucleotide-binding oligomerization domain-like receptor family pyrin domain containing 3 (NLRP3) inflammasome is also activated in response to cholesterol crystals and oxLDL, amplifying inflammatory cascades through increased IL-1β production [177]. Over time, this cycle of lipid deposition, oxidative stress, and inflammation leads to plaque growth, calcification, and the potential for plaque rupture, which can result in acute CVDs such as myocardial infarction or stroke [178].

MOFs, characterized by their high porosity, can serve as carriers of anti-ROS and anti-inflammation drugs. Sheng et al. reported the first MOF-based approach for treating atherosclerosis using an *in-situ* method to encapsulate losartan potassium within the ZIF-8 framework. The ZIF-8 framework, known for its pH sensitivity, allows the acidic environment within atherosclerotic plaques to disrupt its coordination structure, resulting in the controlled release of losartan potassium. As an angiotensin II receptor blocker, losartan potassium inhibits angiotensin II-induced ROS production and the secretion of proinflammatory cytokines, such as IL-6, IL-1β, and TNF-α, all of which contribute to plaque formation. Additionally, ZIF-8 has been shown to induce autophagy in foam cells, promoting reverse cholesterol transport and thereby preventing or reversing lipid accumulation within atherosclerotic plaques. The effectiveness of this design was validated using an $ApoE^{-/-}$ mouse model [37].

During atherosclerosis development, antioxidant enzymes, including SOD and GPx, are often found to be deficient, contributing to oxidative stress and further accelerating disease progression. MOF-based nanozymes with ROS-scavenging activity can be directly applied in treating atherosclerosis. Liu et al. synthesized MIL-53(Fe)-X@Se nanozymes (X = NH_2, F, OH, NO_2, H) using a one-pot synthesis method, incorporating varying amounts of selenium (Se) nanoparticles into the MOF precursor. The resulting nanozymes possess anti-senescence and antioxidant properties, as Fe-MOF exhibits SOD-like activity and Se nanoparticle exhibits GPx-like activity, both of which effectively scavenge ROS. By removing ROS, the nanozyme protects endothelial cells from oxidative-stress-induced senescence; it reduces DNA damage, as indicated by lower phosphorylated H2A histone family member X levels (γ-H2AX) and downregulates the senescence marker $p16^{INK4a}$, thereby attenuating cellular aging. Moreover, its GPx-like activity prevented LDL oxidation and foam cell formation in atherosclerosis. After intravenous administration, the designed nanozymes effectively prevented the progression of atherosclerosis in $ApoE^{-/-}$ mice by attenuating senescent cell

accumulation and reducing oxidative stress and inflammation within atherosclerotic plaques [122].

Combining the targeting properties with the drug-loading capabilities of MOFs is crucial for more precise treatment. The Li and Lu group reported the use of UiO-66-NH_2 as a loading and functional MOF due to its exceptional stability in water and degradability in phosphate-buffered solution, making it highly suitable for biomedical applications. To enable fluorescence tracking, they functionalized the UiO-66-NH_2 by attaching 5-carboxyfluorescein (5-FAM) via the amino group on the MOF's ligand. Rapamycin, a potent immunosuppressant and mTOR pathway inhibitor used in the treatment of atherosclerosis, was then loaded into the UiO-66-NH_2 framework. Subsequently, the interleukin-1 receptor antagonist (IL-1Ra) was conjugated to the rapamycin-loaded MOF. IL-1Ra targets interleukin-1 receptor type I (IL-1RI), blocking its interaction with proinflammatory IL-1, thereby suppressing classically activated (M1) macrophages and promoting tissue repair by inducing alternatively activated (M2) macrophages. In the release medium, phosphate ions exchange with the ligand in UiO-66-NH_2, disrupting the MOF structure and triggering the controlled release of rapamycin. However, rapamycin alone has limitations as a monotherapy due to its tendency to promote M1 macrophage polarization, which can exacerbate inflammation. By combining rapamycin with IL-1Ra, this approach mitigates the pro-inflammatory response induced by rapamycin, while simultaneously promoting M2 macrophage polarization. This synergistic strategy shows significant potential for enhancing atherosclerosis treatment by effectively suppressing inflammation and promoting tissue regeneration [124].(Fig. 4A) Later, they reported using ZIF-8 as a drug carrier to load thiamine pyrophosphate, a known antagonist of the macrophage-overexpressed P2Y6 receptor, which contributes to lipid uptake during the progression of atherosclerosis. The controlled release of thiamine pyrophosphate from ZIF-8 inhibited macrophage lipid uptake and disrupted lipid metabolism via the PI3K/AKT pathway, demonstrating a strong anti-atherosclerotic effect [125]. Liu et al. employed a one-pot synthesis method to encapsulate anti-miR155 within ZIF-8 and coat it with neutrophil membranes, which contain CD18. The neutrophil membrane coating facilitates targeted delivery of anti-microRNA-155 (anti-miR-155) loaded ZIF-8 nanoparticles to endothelial cells in atherosclerotic lesions via the specific binding of CD18 on the nanoparticle surface to ICAM-1 expressed on endothelial cells. Upon cell uptake, the designed nanoparticles were transported into the acidic environment of endosomes and lysosomes, where the coordination bonds in ZIF-8 were broken, resulting in the release of anti-miR155 into the cytoplasm. Therefore, there was a decrease in the levels of miR-155, a crucial regulator of inflammation in atherosclerosis, leading to the restored expression of its target gene, B-cell lymphoma 6 (BCL6). This restoration subsequently suppressed the expression of RELA, a pro-inflammatory component of nuclear factor kappa B (NF-κB), along with its downstream inflammatory targets, ICAM-1 and C—C motif chemokine ligand 2 (CCL2), in endothelial cells [123] (Fig. 4B).

Tang's group developed a series of atherosclerosis diagnostic nanosensors based on PCN-224, utilizing their two-photon fluorescence imaging capability. This approach benefits from reduced biological background interference and enhanced tissue penetration, providing a new way to evaluate early-stage atherosclerosis progression in mice. The fluorescence nanosensor is designed to detect changes in protein phosphorylation levels, as the porphyrin ligand in PCN-224 can be replaced by phosphate. This substitution occurs due to the strong coordination interaction between the hard base of phosphate and the hard metal Zr in accordance with Pearson's hard and soft acids and bases principle [158]. As the phosphorylation level increases in the atherosclerotic model, more porphyrin ligands are exchanged, and phosphate disrupts the charge transfer between the Zr metal ion and the porphyrin molecules within the PCN-224 structure. This disruption causes fluorescence quenching at 507 nm, while a strong fluorescence enhancement occurs at 645 nm due to the restoration of porphyrin fluorescence when excited at 415 nm [38]. In their subsequent work, a dual molecular detection system was developed by attaching a pH-sensitive piperazine moiety (NP-HPZ) to the exterior surface of PCN-224 to simultaneously detect pH and protein phosphorylation levels [91]. Later, they also incorporated iodine (I_3^-)-rhodamine B (RhB) into the PCN-224 structure to measure glucose and protein phosphorylation levels together in the atherosclerotic mice [90]. The PCN-224-NP-HPZ dual detection system demonstrated decreased blood and tissue pH levels and significantly elevated phosphate and phosphorylation levels during the early stages of atherosclerosis compared to healthy mice. Furthermore, their I_3^--RhB@PCN-224 dual detection system indicated that protein phosphorylation and glucose levels in the blood were elevated in early-stage atherosclerotic mice compared to normal mice.

MOF-based theranostic agents that integrate nanozyme activity, drug-loading capacity, targeting ability, and diagnostic functionality are considered promising solutions for the treatment of atherosclerosis. Lv et al. developed such a system by loading curcumin (Cur), an anti-atherosclerosis agent into PCN-222(Mn) and subsequently functionalizing the PCN-222 with dextran sulfate, which can bind to SR-A on the surface of macrophage, particularly those in atherosclerotic plaques. The Mn-based PCN-222 exhibited both SOD- and POD-like nanozyme activities, as confirmed by electron spin resonance (ESR) analysis, effectively enabling the neutralization of superoxide anions and hydroxyl radicals (·OH). When Cur/PCN-222@dextran sulfate was taken up by lipopolysaccharide (LPS)-activated RAW264.7 macrophages in vitro, its SOD-like function rapidly depleted intracellular superoxide, and the resulting H_2O_2 was further reduced—either by the MOF's POD-like activity or by Cur's GPx-mimetic activity—thereby lowering overall ROS levels. Lower ROS levels shifted macrophages from a proinflammatory M1 phenotype to an M2 phenotype. This repolarization suppressed redox-dependent transcription of TNF-α, monocyte chemoattractant protein-1 (MCP-1), and IL-1β, reducing oxidative stress-induced apoptosis and downstream inflammatory signaling. In addition, with ROS elimination, the Liver X receptor alpha (LXRα)/ATP-binding cassette transporter A1 (ABCA1) pathway was reactivated, autophagy was restored, and oxLDL-driven foam-cell formation was prevented. Because dextran sulfate targets SR-A, both the MOF carrier and the curcumin payload were efficiently delivered to the plaque sites. The nanozyme activity, combined with the controlled release of curcumin, resulted in enhanced ROS scavenging, thereby reducing inflammation and lipid accumulation, ultimately leading to a reduction in plaque area. Additionally, the integration of Mn as the metal node in the MOF's framework endowed the platform with MRI contrast capabilities as a T_1 contrast agent, enhancing imaging on both 3 T and 1 T MRI machines, with longitudinal relaxation rates of 33.71 mmol L^{-1} s^{-1} at 3 T and 7.01 mmol L^{-1} s^{-1} at 1 T. As a result, brighter imaging of the aorta was observed in ApoE$^{-/-}$ mice 30 min after injection of Cur/MOF@-dextran sulfate (Fig. 4C) [68]. Li et al. also developed a combined theranostic agent by loading NLRP3 counteracted siRNA (siNLRP3) into MIL MOF (MIL-53(Fe) and MIL-100(Fe)), followed by post-synthetic functionalization with a multifunctional, custom-designed polymer, poly(butyl methacrylate-*co*-methacrylic acid) branched phosphorylated β-glucan (PBMMA-PG). The hydroxy groups in PBMMA-PG were coordinated to the open metal sites within the MOF structure, while the β-glucan component was utilized to target Dectin-1$^+$ macrophages, and PBMMA was incorporated to enhance endosomal escape for efficient gene delivery. The released siNLRP3 effectively suppressed NLRP3 expression and subsequent inflammasome activation, leading to a decreased production of IL-1β. The Fe in the MOF structure was demonstrated to exhibit T_1 contrast properties in 7 T MRI machine. The highest imaging enhancement was observed six-hour post-injection, with lower contrast levels recorded in the control group and at 24 h post-injection. Additionally, Fe in the MOF structure acted as a POD-like nanozyme and exhibited ROS scavenging activity as shown by 2′,7′-dichlorodihydrofluorescein diacetate (DCFH-DA) assays in LPS-activated RAW264.7 macrophages and by dihydroethidium (DHE) staining in aortic root cross-sections, thereby contributing to the

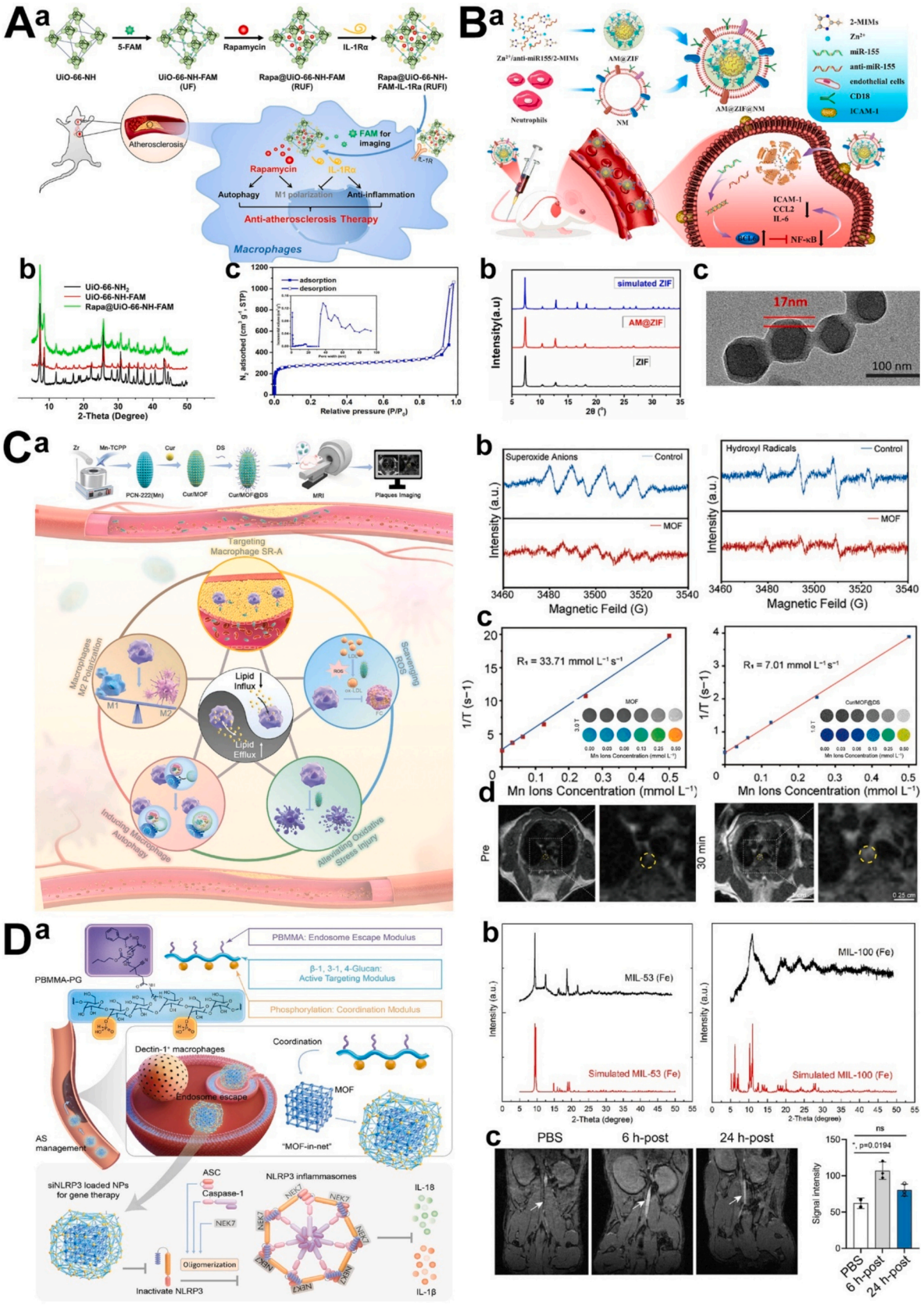

(caption on next page)

Fig. 4. (A) (a) Schematic of the Rapa@UiO-66-NH-FAM-IL-1Ra (RUFI) preparation process and the potential mechanism of anti-atherosclerosis therapy; (b) Powder X-ray diffraction (PXRD) patterns of a series of as-synthesized materials; (c) N_2 adsorption isotherms for the as-synthesized UiO-66-NH_2 [124]. Reproduced with permission. Copyright 2023, *J. Controlled Release*. (B) (a) Schematic illustration of the anti-atherosclerosis targeted treatment by using neutrophil-membrane-coated anti-miR-155-loaded ZIF-8 nanoparticles (AM@ZIF@NM NPs); (b) PXRD patterns of simulated ZIF-8, pure ZIF-8 and AM@ZIF; (c) TEM images of AM@ZIF@NM [123]. Reproduced with permission. Copyright 2023, *ACS Nano*. (C) (a) Schematic illustration of Cur/MOF@dextran sulfate for treatment and enhanced MRI of atherosclerosis; (b) ESR spectroscopy detection of the scavenging ability of MOF for ·OH and superoxide anions; (c) Functional relationship between the Mn concentration and 1/T of MOF; (d) T_1-weighted MRI of the aorta before and after tail vein injection of Cur/MOF@DS after 30 min. The areas shown in the circle were contrast-enhanced regions of atherosclerotic plaque on MRI [68]. Reproduced with permission. Copyright 2024, *Adv. Sci*. (D) (a) Conceptual schematic of the nanoparticle fabrication and therapeutic principle underlying its design; (b) PXRD analysis to characterize the crystalline structures of Fe-based MOF; (c) Representative MRI images and quantified signal intensity post GAMMA-53 nanoparticles injection [126]. Reproduced with permission. Copyright 2025, *Bioact. Mater*.

reduction of oxidative stress associated with atherosclerosis [126]. (Fig. 4D).

3.2. Thrombosis

Thrombosis and its associated complications account for nearly 30 % of annual deaths [128]. Arterial thrombosis can partially or fully block blood vessels, making it a leading cause of life-threatening conditions such as ischemic stroke, mesenteric ischemia, and myocardial infarction. Thrombus therapy primarily focuses on the removal of clots to restore normal blood flow [179]. Zheng et al. reported a targeted dual-modality photothermal/photodynamic thrombolysis strategy using a carbonized ZIF-8@mSiO_2 core-shell structure to produce porphyrin-like mesoporous carbon nanospheres. These nanospheres were functionalized with Arg-Gly-Asp (RGD)-vitamin E–poly(ethylene glycol)–COOH (RGD-PMCS). The RGD peptide enables selective targeting of glycoprotein IIb/IIIa receptors on the surface of activated platelets, minimizing the bleeding risks associated with systemic fibrinolytic therapy. PDT is facilitated by the generation of ROS from the porphyrin moiety of the nanocomposite under NIR laser irradiation. It damages platelet factor 3, through inducing lipid peroxidation, thereby inhibiting thrombus recurrence. Combining PDT and PTT under NIR laser irradiation enhances the thrombus-clearing efficiency [32]. (Fig. 5A) Zhang et al. also reported the carbonization of MIL-101(Fe) to produce carbon nanoparticles, with Fe metal node from the MIL-101 combined with oxygen atoms in the atmosphere, resulting in the formation of magnetic iron oxide. This magnetic iron oxide nanoparticle enables magnetothermal thrombosis treatment under an alternating magnetic field, while the carbon nanoparticles formed during carbonization are used for photothermal thrombolysis under NIR radiation. uPA, a thrombolytic agent, can be electrostatically absorbed onto the surface and within the pores of the carbonized nanoparticles. This dual system, combining NIR-triggered uPA release with the magnetothermal effect, demonstrated thrombolytic efficiency six times higher than that achieved by NIR treatment alone [127].

Chiang et al. reported a targeted combined therapy for thrombus treatment that integrate phototaxis, photosynthesis, and magnetothermal therapy. Iron oxide nanoparticles were encapsulated within MIL-101, and uPA was loaded inside the MOF pores. Fucoidan (F) and glycol chitosan (GCS) were attached to the outer surface of the MOFs. The resulting nanoparticles were taken up by *Chlamydomonas reinhardtii* (CHL), a microalga capable of phototactic targeting of thrombi under a 522 nm laser and generating oxygen via photosynthesis when exposed to a 632 nm laser. The iron oxide nanoparticles inside the MOF enable magnetothermal therapy by increasing the temperature under an alternating magnetic field, thereby enhancing the release of uPA [129]. Yuan et al. also reported the use of a targeted bioMOF therapeutic agent for thrombolysis, where CD-MOFs serve as the shell to coat $CaCO_3$/polydopamine (CP) nanoparticles, called $CaCO_3$/PDA@CD-MOFs (MC). The RGD peptide is attached to the outer surface of the MOF to enable selective targeting of glycoprotein IIb/IIIa receptors on activated platelets. UPA and acetylsalicylic acid (ASA), an anti-inflammatory drug, both used in the treatment or prevention of venous thromboembolism, were co-loaded into the core-shell structure. The authors claimed that the macromolecule uPA can be safely adsorbed within the MOF's pore structure, while the smaller ASA molecule is loaded into the cyclodextrin cavity in the shell. The CP nanoparticle is pH-responsive and undergoes decomposition in the ischemic inflammatory environment, leading to the disintegration of MC. This rapid disintegration facilitates the quick release of uPA, enabling effective thrombolysis. Meanwhile, ASA is gradually released to inhibit platelet aggregation and alleviate inflammation, contributing to sustained anti-thrombotic effects (Fig. 5B) [94].

Cao et al. reported a pioneering approach utilizing piezoelectric materials for thrombosis theranostics, integrating piezoelectrodynamic therapy, Fenton reactions, chemiluminescence-excited PDT, and thrombus targeting. They first modified tetragonal barium titanate (tBT) nanoparticles with carboxyl groups to facilitate encapsulation. These surface-functionalized nanoparticles were then introduced into a solution containing MOF precursors, $FeCl_3$ and benzene-1,3,5-tricarboxylic acid, forming a core-shell tBT@MOF structure. Chlorin e6 (Ce6)-luminol conjugates (Ce6-Lum) were loaded into the MOF pores, and the surface of the MOF was functionalized with heparin to form the tBT@MOF_{CL}/Hep nanoparticle. The heparin on the surface spontaneously targeted thrombi, promoting nanoparticle accumulation and exerting an anticoagulant effect. Thrombosis generates significantly higher endogenous shear stresses, which increase cubically as the vessel diameter decreases. The tBT@MOF_{CL}/Hep nanoparticles were stretched or torn by shear stress in vascular stenosis. As a result, the tBT nanoparticles in the tBT@MOF_{CL}/Hep structure converted mechanical energy into chemical energy by transferring electrons, which react with surrounding water and oxygen to produce ROS. This electron transfer reduces Fe^{3+} in the MOF structure to Fe^{2+}, facilitating the Fenton reaction, where Fe^{2+} catalyzes the H_2O_2 to generate additional ROS. This process leads to the breakdown of the MOF structure, releasing Ce6-Lum, while the luminol is oxidized by ROS to emit blue light. The emitted blue light excites Ce6, generating red fluorescence to enable thrombus detection. The generated ROS could be used for thrombolysis (Fig. 5C) [128].

The above studies by Zheng [32] and Cao [128] primarily focus on generating ROS for thrombolysis. However, the amount of ROS generated at the thrombus site by damaged endothelial cells and activated platelets is approximately double that of healthy vessels. This elevated ROS level exacerbates vascular injury and heightens the risk of thrombotic complications by promoting platelet aggregation and accelerating thrombus formation. This underscores the importance of integrating ROS-scavenging approaches into the thrombus microenvironment to enhance the efficacy of thrombolytic treatment. To address this, Shan et al. reported a CAT nanozyme, Ce-UiO-66, designed specifically to scavenge ROS. The MOF was coated with mesenchymal stem cell (MSC) membranes expressing CD18 molecules. Since CD18 specifically binds to ICAM-1, which is highly expressed on inflamed or thrombotic endothelial cells, the MSC membrane coating enabled targeted accumulation of the nanozyme at inflammatory endothelial sites. Upon successful targeting, the coexistence of Ce (III) and Ce (IV) in the Ce-UiO-66 structure provides catalytic activity, facilitating the decomposition of H_2O_2 to generate oxygen, thereby exhibiting CAT-like activity. With the assistance of ultrasound, this system achieves rapid and precise thrombolytic therapy. The authors also highlight that the MOF's porous structure enables the generation of electron holes, which act as micro-

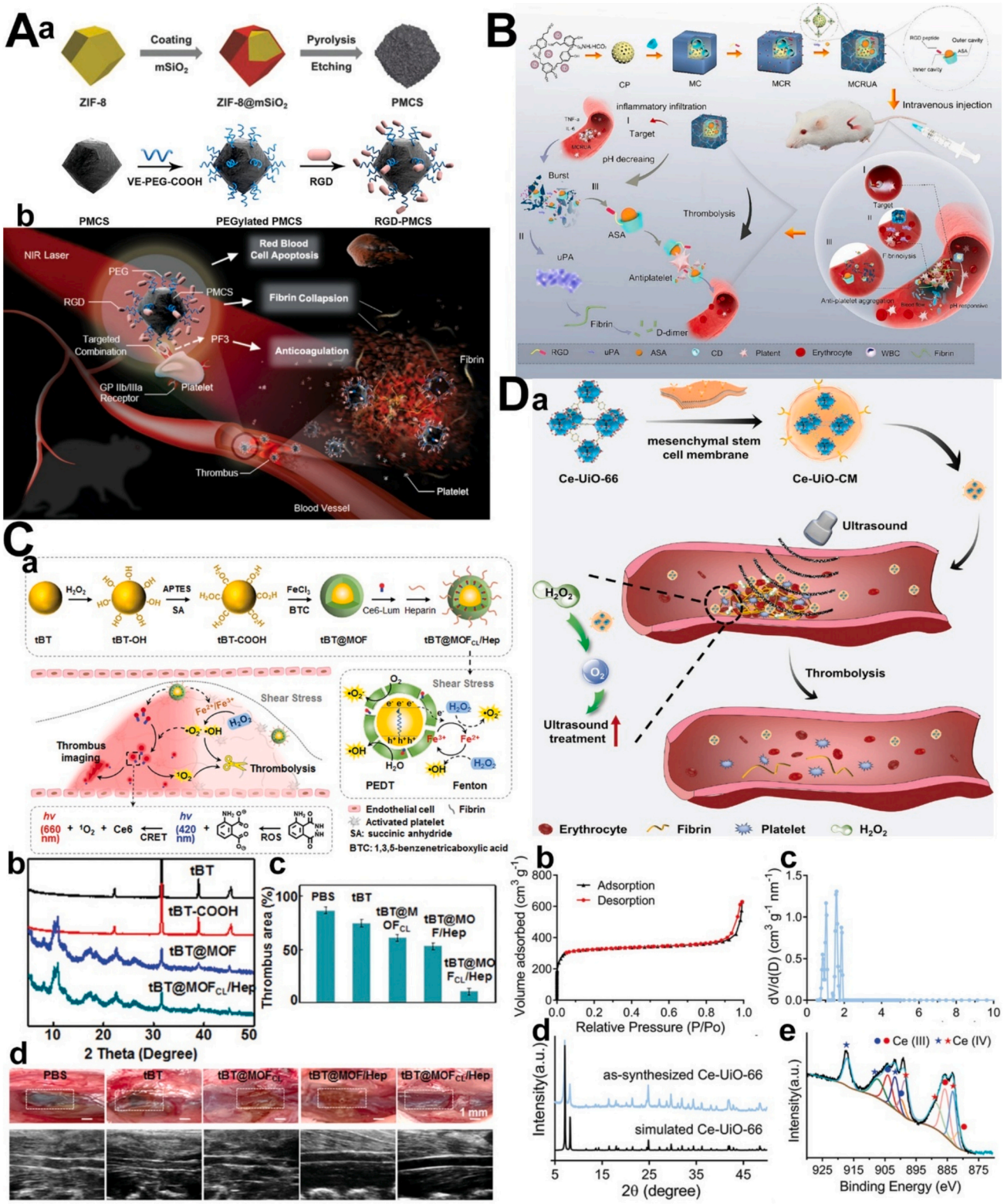

Fig. 5. (A) (a) The synthesis process of PMCS and mesoporous carbon nanospheres [180] and RGD-PMCS synthesis; (b) Schematic illustration of RGD-PMCS-mediated site-specific photothermal/photodynamic thrombus therapy [32]. Reproduced with permission. Copyright 2018, *Adv. Mater.,* and Copyright 2019, *Adv. Sci.* (B) Design of $CaCO_3$/PDA@CD-MOFs-RGD/uPA/ASA for venous thromboembolism [94]. Reproduced with permission. Copyright 2024, *Carbohydr. Polym.* (C) (a) Schematic illustration of the preparation process and thrombolysis mechanism of tBT@MOF_{CL}/Hep; (b) PXRD patterns of tBT, tBT-COOH, tBT@MOF and tBT@MOF_{CL}/Hep; (c) the qualified thrombolytic rates after treatment with different nanoparticles; (d) visual and doppler ultrasound images for in vivo thrombus imaging and thrombolysis evaluation [128]. Reproduced with permission. Copyright 2023, *Adv. Funct. Mater.* (D) (a) Schematic illustration of the synthesis of Ce-UiO-cell membrane and its application in thrombolytic therapy in combination with ultrasound; (b) N_2 sorption isotherm of Ce-UiO-66.; (c) the corresponding pore size distribution of Ce-UiO-66 was calculated by the DFT method; (d) PXRD patterns of simulated Ce-UiO-66 and as-synthesized Ce-UiO-66; (e) the magnified Ce 3d X-ray photoelectron spectroscopy (XPS) spectrum of Ce-UiO-66 [130]. Reproduced with permission. Copyright 2024, *Adv. Sci.*

reactors to further enhance its ROS-scavenging activity (Fig. 5D) [130].

3.3. Myocardial infarction

Myocardial infarction, caused by the occlusion of a coronary artery, represents the most severe form of CVD [181]. Reduced blood flow to the heart triggers ischemia, hypoxia, and irreversible myocardial cell death, which in turn triggers an intense inflammatory response and excessive ROS production, further amplifying injury to the infarcted myocardium [182]. The involvement of ROS in myocardial infarction spans both early and late stages, initiating apoptosis and necrosis during the acute phase and facilitating oxidative stress-mediated fibrosis and ventricular remodeling in the chronic phase. These excessive ROS mediate inflammatory and pro-apoptotic signaling, as well as extracellular matrix remodeling, exacerbating myocardial injury [183]. Consequently, the elimination of excess ROS is widely acknowledged as an effective strategy for protecting the myocardium. Guo et al. used UiO-66 to immobilize natural SOD on its surface, applying it for efficient ROS scavenging. They were the first group to use a MOF-based approach in the therapy of acute myocardial infarction [35]. Xiang et al. reported a bimetallic MOF nanozyme (Cu-TCPP-Mn) by incorporating Mn^{2+} to replace partially Cu^{2+} in the Cu-TCPP MOF, forming a two-metal MOF structure. The nanozyme mimics SOD and CAT activities, converting oxygen radicals into H_2O_2 through SOD mimicry, followed by CAT

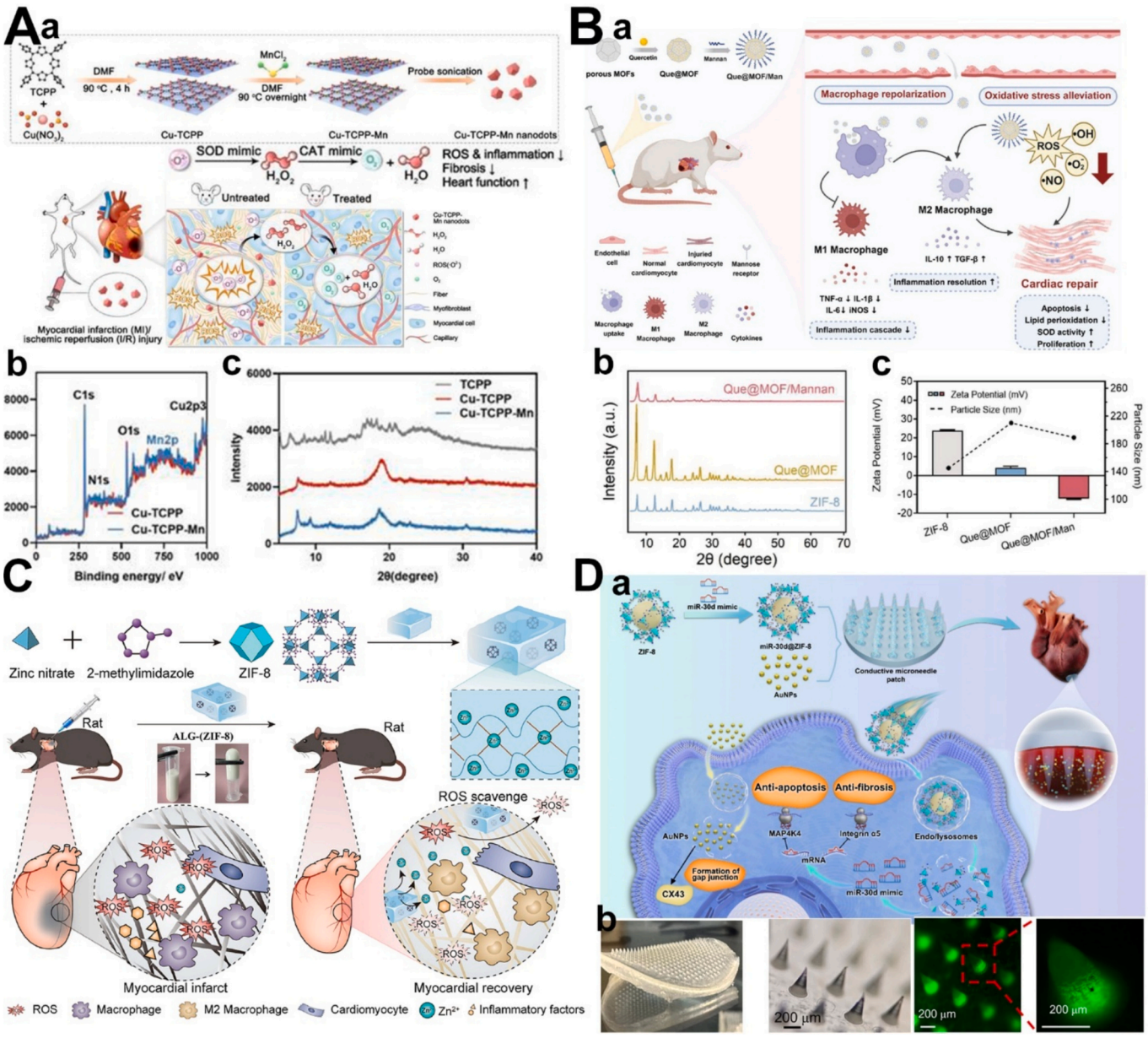

Fig. 6. (A) (a) Schematic illustration of the design and synthesis of Cu-TCPP-Mn nanozyme for myocardial injury treatment; (b) XPS spectra of Cu-TCPP and Cu-TCPP-Mn; (c) PXRD patterns of the TCPP, Cu-TCPP and Cu-TCPP-Mn [89]. Reproduced with permission. Copyright 2023, *Theranostics*. (B) (a) Schematic illustration of the inflammation-targeting Que@MOF/Man nanoparticles for antioxidant and anti-inflammatory treatment against myocardial infarction injury: (b) PXRD patterns of Que@MOF/Man, Que@MOF, and ZIF-8; (c) zeta potential and particle size for Que@MOF/Man, Que@MOF, and ZIF-8 measured using dynamic light scattering [134]. Reproduced with permission. Copyright 2024, *Adv. Sci.* (C) (a) Schematic illustration of the design and synthesis of ALG-(ZIF-8) nanozyme hydrogel for myocardial infarction treatment [82]. Reproduced with permission. Copyright 2024, *Acta Biomater*. (D) (a) A conductive microneedle patch and miR-30d nanodelivery system are integrated to alleviate myocardial ischemia–reperfusion injury; (b) digital photograph of the entire conductive microneedle patch, microscopic images of the patch, and fluorescence microscopy images of the conductive microneedle [133]. Reproduced with permission. Copyright 2024, *ACS Nano*.

mimicry to catalyze the conversion of H_2O_2 into oxygen and water. Consequently, Cu-TCPP-Mn reduced proinflammatory cytokines (IL-1β, TNF-α) while increasing the anti-inflammatory cytokine IL-10 in LPS-stimulated RAW 264.7 macrophages. It also significantly reduced intracellular ROS levels in H9C2 (rat cardiomyocytes) and improved cell viability after H_2O_2 exposure, demonstrating strong antioxidant and cytoprotective effects in vitro through ROS scavenging. Similarly, Cu-TCPP-Mn treatment rescued infarcted myocardium from ROS-induced apoptosis, as shown by terminal deoxynucleotidyl transferase dUTP nick-end labeling (TUNEL) staining, and promoted long-term ventricular remodeling, enhancing cardiac function and mitigating myocardial damage in preclinical models of myocardial infarction and ischemia-reperfusion injury (Fig. 6A) [89]. Zhong et al. developed a nanozyme that mimicked CAT and SOD by encapsulating ZIF-8 nanoparticles within a sodium alginate hydrogel (ALG). This construction scavenged ROS and repolarized macrophages toward the anti-inflammatory M2 phenotype, thereby neutralizing inflammatory cytokines and promoting vascularization within the infarcted region. Upon hydrogel degradation, Zn^{2+} ions, originating from the ZIF-8 structure were gradually released and subsequently cross-linked with the negatively charged carboxyl groups of ALG. This cross-linking mechanism effectively maintained the Zn^{2+} release concentration below 30 μg/mL, preventing excessive ion release and associated cytotoxicity. Consequently, this controlled, low-dose Zn^{2+} release promoted vascularization and reduced maladaptive ventricular remodeling in the myocardial infarction area (Fig. 6C) [82]. Hu et al. reported a targeted ROS scavenger by loading quercetin (Que) into the ZIF-8 framework and electrostatically attaching mannan (man) to the surface of the MOF. This functionalization enables the designed structure to bind to the carbohydrate recognition domains of mannose receptors, which are highly expressed on macrophages at inflammation sites, thereby promoting nanoparticle endocytosis into the macrophages rather than cardiomyocytes, enhancing targeted therapeutic delivery. Compared to free quercetin, Que@MOF/Man dramatically lowered intracellular ROS levels (as shown by DCFH-DA assays), prevented lipid peroxidation (indicated by decreased malondialdehyde levels), restored SOD activity, and repolarized macrophages to an anti-inflammatory M2 phenotype. This was evidenced by decreased levels of M1 markers (e.g., CD86, inducible nitric oxide synthase (iNOS), IL-1β, IL-6, and TNF-α) and increased levels of M2 markers (e.g., CD206, arginase-1 (Arg-1), and IL-10) at both the transcriptional and protein levels. Que@MOF/Man more effectively created a microenvironment conducive to cardiac repair after myocardial infarction than free quercetin. Consequently, it promoted cardiac repair after myocardial infarction, reduced cardiomyocyte apoptosis, increased proliferation of $cTnT^+$ cardiomyocytes, promoted angiogenesis, and preserved cardiac function in a rat model (Fig. 6B) [134].

Blood reperfusion may exacerbate myocardial injury by inducing secondary cardiomyocyte death and fibrosis, a process referred to as myocardial ischemia−reperfusion injury. MicroRNAs (miRNAs), a class of small RNAs, can regulate mRNA via binding to the complementary sequences to influence the cardiovascular system, playing a crucial role in cardiac repair and regeneration. Chen et al. developed a conductive microneedle patch incorporating ZIF-8-encapsulated miR-30d and gold nanoparticles, enabling localized and sustained delivery of miR-30d to cardiomyocytes. This method ensures deeper penetration into necrotic tissue without being washed away by blood circulation. The gold nanoparticles released from the microneedles enhance electrical conductivity in the infarcted area, promoting the restoration of synchronous contraction and relaxation of the heart muscle. Additionally, ZIF-8 serves as a transfection agent for miR-30d, utilizing the proton sponge effect to facilitate miR-30d's escape from endosomes. This protects the miRNA from degradation and enables successful expression in the myocardium, thereby offering protection against heart failure (Fig. 6D) [133].

3.4. Critical limb ischemia

Critical limb ischemia, the most advanced stage of peripheral artery disease, is primarily caused by atherosclerosis, which leads to significant blood flow reduction in the limbs. Critical limb ischemia is associated with poor functional outcomes, a high risk of amputations, and a 5-year mortality rate of up to 60 %, making it a significant public health issue [184,185]. Approximately 40 % of critical limb ischemia patients are not eligible for open or endovascular revascularization procedures due to factors such as severe comorbidities, poor vascular anatomy, infections, and non-healing ulcers [186]. Therefore, therapeutic angiogenesis has been widely applied to improve blood perfusion in affected limbs by promoting the development of new blood vessels or by restoring balance in the ischemic microenvironment through the alleviation of excessive inflammation and oxidative stress [187,188]. Feng's group has reported a series of significant studies utilizing Zn-based MOFs (ZIF-8 and ZIF-90) as effective, facile, and cost-effective agents for therapeutic angiogenesis. Zn^{2+} plays a crucial role in supporting the generation of redox signaling molecules, such as H_2O_2 and $O_2^{-}\cdot$, by mitochondria under ischemic conditions, which is important for survival, proliferation, and migration, critical processes for blood vessel formation [189]. In their initial work, to improve Zn^{2+} availability and reduce the required dose, they attached two targeting peptides, an endothelial-targeting peptide and a mitochondria-localizing-sequence peptide, to the surface of ZIF-90 through a Schiff-base reaction to construct EM-Z90. The endothelial-targeting peptide facilitates ZIF-90 entry into endothelial cells, while the mitochondria-localizing peptide ensures ZIF-90 accumulates in mitochondria. These peptides enable efficient entry and accumulation of ZIF-90 at a very low dosage (0.05 μg/mL), enhancing the expression of key pro-angiogenic regulators such as HIF-1α, VEGF and eNOS, while promoting NO production to support endothelial cell morphogenesis. In a critical limb ischemia mouse model, a superlow dosage of 4.4 μg/kg of EM-Z90, which is approximately an order of magnitude lower than previously reported minimum effective doses, effectively augmented local vascularization in ischemic limbs without causing muscle injury or toxicity (Fig. 7A) [36]. In their subsequent work, they aimed to enhance the intercellular signaling between endothelial cells and macrophages to further promote therapeutic angiogenesis. They developed a one-pot synthesis strategy to load $Mn_2(CO)_{10}$ into the ZIF-8 framework, followed by functionalization with HA-CAG peptide (CAG peptide: amino acid sequence: -NH_2-Cys-Ala-Gly-COOH) via electrostatic interactions. In this process, the carboxyl group of HA reacts with the amino group at the N-terminus of the CAG peptide to form stable HA-CAG peptide. HA binds to the CD44 on macrophages, inducing phagocytosis, while the CAG peptide has high affinity for vascular endothelial cells. Upon intracellular uptake, CO is released from $Mn_2(CO)_{10}$ and Zn^{2+} is released from ZIF-8. These combined releases modulated macrophage polarization toward the anti-inflammatory M2 type and promoted vascular endothelial cell morphogenesis during angiogenesis in ischemic tissues [135]. In their third study, they loaded diallyl trisulfide (DATS), as an H_2S donor into ZIF-8 and functionalized the ZIF-8 surface with HA-PEG-CLS (cholesterol) through electrostatic interactions. After intramuscular injection into the gastrocnemius muscle, the HA-PEG-CLS@ZIF@DATS nanoparticles were phagocytized by macrophages. Due to the lipophilicity of CLS, the nanoparticles interact with the lipid-rich cell membranes of capillary endothelial cells, facilitating their entry. Once inside the cells, the ZIF-8 framework degrades, controlling and slowing the release of H_2S produced from DATS by reacting with cellular thiols, such as glutathione and cysteine. The released H_2S promotes endothelial morphogenesis and macrophage polarization to the M2 phenotype, exhibiting pro-healing, pro-angiogenic, antioxidant, and anti-inflammatory properties [136]. Building on the importance of H_2S in critical limb ischemia treatment, Hu et al. reported that the H_2S-releasing donor GYY4137 (morpholin-4-ium 4-methoxyphenyl(morpholino)phosphinodithioate), a sulfide salt, could be co-encapsulated with

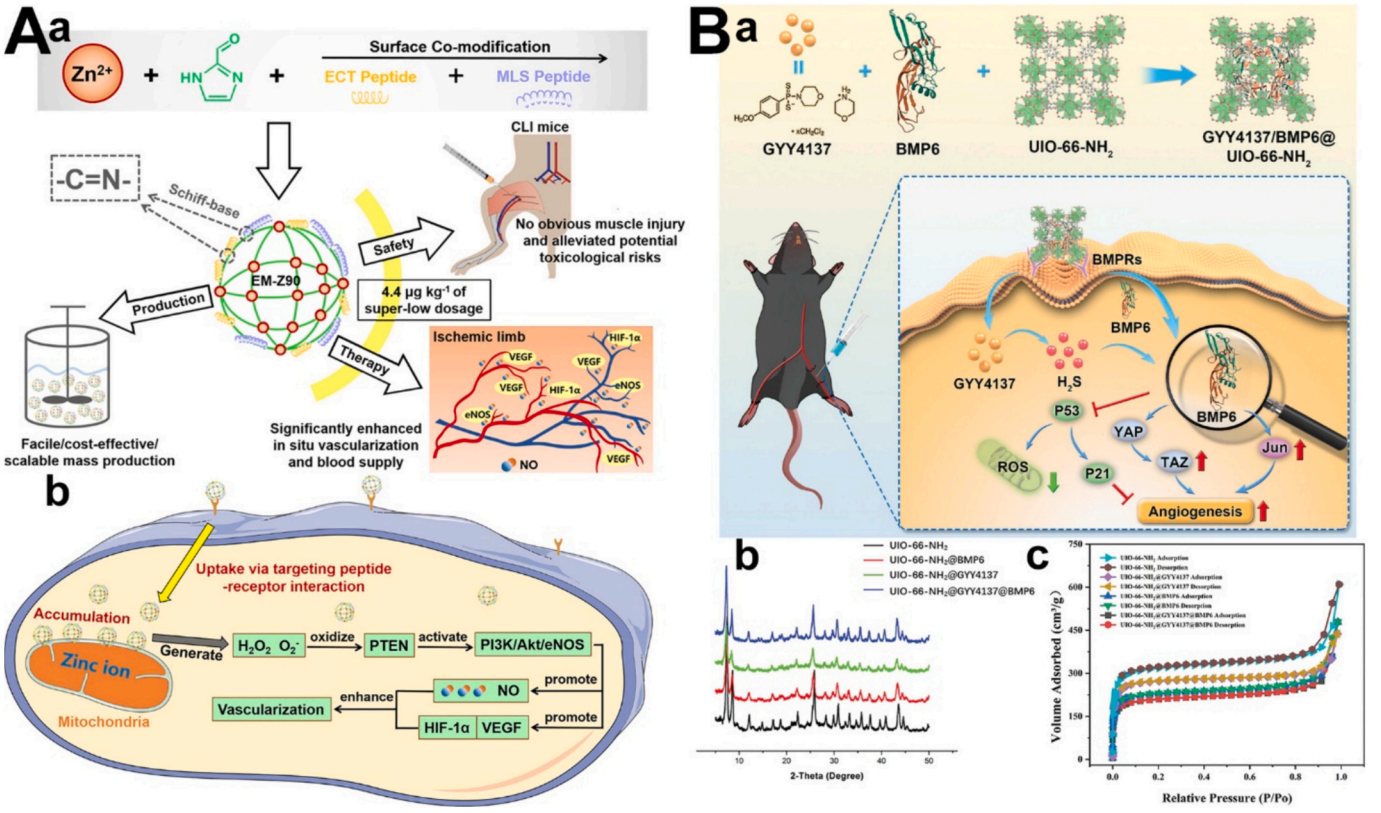

Fig. 7. (A) (a) Illustration of the preparation of EM-Z90 nanomaterial and its comprehensive advantages as an advanced critical limb ischemia drug agent, including superlow dosage, therapeutic efficacy, safety, and suitability for mass production; (b) Inferred working mechanism of Zn-MOFs in intrinsically promoting vascularization [36]. Reproduced with permission. Copyright 2022, *ACS Nano*. (B) (a) Schematic illustration of antioxidant and pro-angiogenic effects and the mechanism of UiO-66-NH_2@GYY4137@BMP6 in treating hindlimb ischemia; (b) PXRD patterns; (c) N_2 adsorption-desorption isotherms [137]. Reproduced with permission. Copyright 2023, *Adv. Healthcare Mater*.

bone morphogenetic protein 6 (BMP6), an angiogenesis-inducing protein, within the UiO-66-NH_2 framework. Following intraperitoneal injection of the designed nanoparticles, H_2S was released in a controlled and sustained manner from the MOF, preventing overproduction of ROS by downregulating the phosphorylation of tumor protein p53 and cyclin-dependent kinase inhibitor 1A (p21). The released BMP6 could enhance therapeutic efficacy by promoting angiogenesis and reducing oxidative stress, enabling effective treatment even at lower doses of GYY4137. This is achieved through the upregulation of phosphorylated Yes-associated protein (YAP)/transcriptional coactivator with PDZ-binding motif (TAZ) and transcription factor AP-1 (Jun) in endothelial cells (Fig. 7B) [137].

Similar to the work by Feng's group, which used ZIF as a controlled and slow-release carrier for Zn^{2+}, Cheng et al. utilized HKUST-1 as a controlled and slow-release carrier for Cu^{2+} for long-term treatment. They employed a one-pot method to encapsulate folic acid into HKUST-1, which was then further encapsulated into a thermoresponsive hydrogel. After injection into the hindlimb muscle, the slow release of Cu^{2+} increased HIF-1α stability by inactivating HIF-1, thereby promoting angiogenesis under ischemic conditions. Since Cu^{2+} can generate ROS, the incorporation of antioxidant folic acid neutralized free radicals and helped mitigate these toxic effects. Folic acid in HKUST-1 reduced ROS levels by approximately 30.3 % in a time-independent manner, ultimately enhancing blood perfusion while minimizing toxicity [79]. Table 3 summarizes recent developments in MOF-based materials for treating various cardiovascular diseases, highlighting synthesis methods, key features, targeted functions, and preclinical evaluations.

3.5. Vascular implants

Vascular implants, such as stents and grafts, have been developed with NO-releasing nanomaterials to treat cardiovascular conditions, including hypertension, atherosclerosis, myocardial ischemia–reperfusion injury, and for applications in cardiac tissue engineering [84]. Cu-based MOFs are widely used in the development of these vascular implant materials due to their ability to catalyze the decomposition of RSNOs to produce NO. This catalytic efficiency is attributed to the well-organized metal-containing nodes in the MOF structure and the pore characteristics of Cu-based MOFs, as summarized in Section 2.1. These MOF-based materials have demonstrated sustained release of NO and Cu ions, while maintaining long-term catalytic performance. NO was catalytically released from nano Cu-MOFs at a physiological flux ($0.5—4 \times 10^{-10}$ mol $cm^{-2}{\cdot}min^{-1}$), closely mimicking the endogenous NO secretion by endothelial cells. This localized NO release effectively stimulated soluble guanylate cyclase (sGC) in platelets, leading to increased intracellular cyclic guanosine monophosphate (cGMP) levels, which in turn inhibited platelet activation and aggregation [190], thereby reducing the thrombogenic potential on the stent surface. Furthermore, under oxidative stress conditions simulated by H_2O_2 exposure, NO exhibited a protective effect on endothelial cells by attenuating ROS-induced apoptosis and reducing the formation of peroxynitrite ($ONOO^-$), which is generated by the reaction between excess NO and free radicals released by activated platelets. This protective effect promoted endothelial cell survival, adhesion, and migration. In addition, Cu ions released from the Cu-MOFs may support endogenous Cu/Zn-SOD activity, contributing to free radical elimination and enhancing endothelial cell viability under oxidative conditions [85]. As a result, these NO-releasing Cu-MOF-based implants exhibit

Table 3
Summary of recent MOF applications in CVDs.

CVDs	MOF	Synthesis Methods	Targeting or functional polymer	Drug or encapsulated material inside	Key design features	Preclinical model	Ref
Atherosclerosis	ZIF-8	One-pot synthesis at room temperature under stirring [119]	None	Losartan potassium	pH-triggered release; autophagy induction	Male ApoE$^{-/-}$ mice	[37]
	PCN-224	Solvothermal synthesis in a Teflon-lined autoclave at 120 °C [120]	Wool-balls	None	Two-photon imaging for protein phosphorylation detection	Male Wistar mice; intraperitoneal injection of vitamin D3; and high-fat diet	[38]
	PCN-224		pH-sensitive piperazine group	None	Dual molecular detection (pH, protein phosphorylation levels) using two-photon fluorescence imaging	Male Wistar mice; intraperitoneal injection of vitamin D3; and high-fat diet	[91]
	PCN-224		None	iodine-rhodamine B	Dual molecular detection (glucose, protein phosphorylation levels) using two-photon fluorescence imaging	Male Wistar rate; intraperitoneal injection of vitamin D3; and high-fat diet	[90]
	MIL-53(Fe)-X (X = NH_2, F, OH, NO_2, H)	Solvothermal synthesis in a Teflon-lined autoclave at 150 °C [121]	None	Se nanoparticle	Nanozyme (SOD-like and GPx-like activity)	Male ApoE$^{-/-}$ mice	[122]
	ZIF-8	One-pot, room-temperature incubation with stirring	Neutrophil membrane	anti-miR155	Endothelial cell targeting; reduces miR-155 levels, a key inflammation regulator in atherosclerosis	Male ApoE$^{-/-}$ mice	[123]
	UiO-66-NH_2	Solvothermal synthesis at 90 °C in a sealed vial	IL-1Ra	Rapamycin	Targeted rapamycin release with IL-1Ra for M2 macrophage induction and M1 macrophage suppression	Male ApoE$^{-/-}$ mice	[124]
	PCN-222(Mn)	Solvothermal synthesis at 120 °C in an oil bath	Dextran sulfate	Curcumin	Targeting curcumin release to macrophages; Mn in the MOF as T_1-weighted MRI contrast agents	Male ApoE$^{-/-}$ mice	[68]
	ZIF-8	One-pot synthesis at room temperature under stirring	None	Thiamine pyrophosphate	Controlled thiamine pyrophosphate release inhibits macrophage lipid uptake and reduces PI3K/AKT pathway activation	Male ApoE$^{-/-}$ mice	[125]
	MIL-53(Fe) and MIL-100 (Fe)	Solvothermal synthesis in a Teflon-lined autoclave at 150 °C for MIL-53 [107] and 200 °C for MIL-100 [21, 185]	PBMMA-PG	siNLRP3	Targeting gene delivery to Dectin-1^{+} macrophages; siNLRP3 release inhibits NLRP3 inflammasome activation and reduces IL-1β; Fe in MOF as T_1-weighted MRI contrast agent.	Male ApoE$^{-/-}$ mice	[126]
Thrombosis	MOF-derived porphyrin-like mesoporous Carbon Nanospheres	Pyrolysis of ZIF-8@$mSiO_2$ at 800 °C under nitrogen	RGD attached vitamin E–poly (ethylene glycol)–COOH	None	Targeting glycoprotein IIb/IIIa receptors on the surface of platelets; ROS generated under NIR laser; combining PDT and PTT with NIR laser	Thrombosis rat model (Male Sprague-Dawley)	[32]
	Carbonized MOFs (Fe)	Carbonization of Fe-MOF at 700 °C under argon	None	uPA	Photothermal thrombolysis under NIR radiation; magnetothermal effects under an alternating magnetic field; drug release	Thrombosis rat model (Sprague–Dawley)	[127]
	Fe-MOF	Solvothermal synthesis in a Teflon-lined autoclave at 120 °C	Heparin	Tetragonal barium titanate nanoparticles and Chlorin e6-luminol conjugates	Heparin on the surface targeted thrombi; Piezoelectrodynamic therapy; Fenton reaction; chemiluminescence-excited PDT and thrombus targeting	Thrombosis rat model (Sprague–Dawley)	[128]
	Fe_3O_4@MIL-100	Microwave-assisted synthesis at 150 °C	Glycol chitosan, fucoidan and *Chlamydomonas Reinhardtii* micromotors	uPA	Targeting of thrombi; phototactic under a 522 nm laser; generates oxygen via photosynthesis when exposed to a 632 nm laser; magnetocaloric therapy.	Carrageenan-induced thrombus in mice	[129]

(*continued on next page*)

Table 3 (*continued*)

CVDs	MOF	Synthesis Methods	Targeting or functional polymer	Drug or encapsulated material inside	Key design features	Preclinical model	Ref
	Ce-UiO-66	Solvothermal synthesis at 80 °C	Mesenchymal stem cell membranes	None	Nanozyme, targeting ICAM-1 vascular endothelium in the thrombosis area, ultrasound therapy	Thrombosis rat model (Sprague-Dawley)	[130]
	CD-MOF	Methanol vapor-diffusion crystallization at room temperature, then ethylene glycol diglycidyl ether crosslinking in ethanol at 65 °C [131]	RGD	uPA and acetylsalicylic acid	Controlled release; targeting glycoprotein IIb/IIIa receptors on the surface of platelets	$FeCl_3$-induced thrombus model in male Kunming mice	[94]
Myocardial infarction	ZIF-8	One-pot synthesis at room temperature under shaking	Silk fibroin assembled into quercetin	None	pH-responsive quercetin release	Myocardial infarction rat model (Sprague-Dawley rats)	[132]
	Zr-MOF	Solvothermal synthesis at 120 °C	None	SOD	Reduces ROS-induced damage caused by hypoxia	Myocardial infarction mouse model (C57BL/6)	[35]
	Cu, Mn- TCPP MOF	Solvothermal synthesis at 90 °C in an oil bath, followed by metal exchange to partially replace Cu with Mn	None	None	Mimics SOD and CAT	Myocardial infarction mice model (C57BL/6) and rat myocardial ischemia−reperfusion injury model	[89]
	ZIF-8	One-pot synthesis at room temperature under stirring	none	miR-30d	MOF as a protection and transfection agent for miR-30d	Mice reperfusion injury model (C57BL/6)	[133]
	ZIF-8	One-pot synthesis at room temperature under stirring	Mannan	Quercetin	Targeting macrophages at inflammation sites, quercetin-controlled release.	Myocardial infarction rat model (Sprague-Dawley rats)	[134]
	ZIF-8	One-pot synthesis at room temperature under stirring	ALG	None	Mimics SOD and CAT and Zn^{2+}-controlled release	Myocardial infarction model in Sprague-Dawley rats	[82]
	CD-MOF	One-pot assembly of γ-cyclodextrin /KOH in water at 60 °C, followed by the addition of PEG_{20000}/MeOH under stirring	Trans-sodium crocetinate	None	Oral delivery system	Beagle dogs and chronic heart failure rats with reduced ejection fraction (male Sprague-Dawley rats)	[95]
Critical limb ischemia	ZIF-90	One-pot synthesis at room temperature under stirring	Endothelial cells-targeting peptide and mitochondria-localizing-sequence peptide	None	ROS are generated under ischemic conditions; NO production; Zn^{2+}-controlled release	Critical limb ischemia mouse model (C57BL/6)	[36]
	ZIF-8	One-pot synthesis at room temperature under stirring	HA-CAG	$Mn_2(CO)_{10}$	CO and Zn^{2+} release and targeting macrophages	Critical limb ischemia mouse model	[135]
	ZIF-8	One-pot synthesis at room temperature under stirring	HA-PEG-CLS	DATS	H_2S and Zn^{2+} release and targeting macrophages	Critical limb ischemia mouse model (male Balb/c)	[136]
	UiO-66-NH_2	Solvothermal synthesis at 90 °C in the vial	None	GYY4137 and BMP6	H_2S controlled release; BMP6 promotes angiogenesis and reduces oxidative stress	Critical limb ischemia mouse model (C57BL/6)	[137]
	HKUST-1	Room-temperature one-pot reaction in DMSO/EtOH/H_2O (2:1:1 *v*/*v*/*v*)	Thermoresponsive hydrogel	Folic acid	Cu^{2+} release promotes angiogenesis under ischemic conditions and folic acid for ROS scavenging	Unilateral hindlimb ischemia mouse model (Male C57BL/6 mice)	[79]

(*continued on next page*)

Table 3 (*continued*)

CVDs	MOF	Synthesis Methods	Targeting or functional polymer	Drug or encapsulated material inside	Key design features	Preclinical model	Ref
Heart defect prevention	Defective UiO-66	Solvothermal synthesis at 220 °C in an oil bath with concentrated HCl added for defect structure	None	Chloroquine diphosphate	Chloroquine diphosphate release from defective UiO-66	*Danio rerio* Model Organism	[138]
Hypertension	MIL-88B	One-pot synthesis at room temperature under stirring	None	NO-releasing complex [Fe_2(μ-$SCH_2CH_2COOH)_2$ $(NO)_4$] (DNIC-2)	When orally administered, the 1,4-benzenedicarboxylate MOF ligand in the DNIC@MOF structure becomes protonated in gastric fluid, triggering its transformation and controlled release of NO in the intestine.	Spontaneously Hypertensive rats	[139]
Abdominal aortic aneurysm therapy	Mn^{2+} doping UiO-66-NH_2	Solvothermal synthesis at 90 °C in the vial followed by metal exchange to partially replace Zr with Mn at 85 °C under stirring	None	Hyaluronate tetrasaccharide	Hyaluronate tetrasaccharide was loaded into the MOF framework to promote vascular smooth muscle cell repair and extracellular matrix remodeling by enhancing contractility and lysyl oxidase activity, while Mn^{2+} in the MOF framework inhibited matrix metalloproteinases, preventing extracellular matrix degradation, and supporting tissue repair	Abdominal aortic aneurysm therapy mouse model using ApoE−/− mice with surgical implantation of a micro-osmotic pump to deliver angiotensin II continuously over 28 days	[140]

antithrombotic effects, promote endothelial cell growth, and reduce neointimal hyperplasia. This makes them promising candidates for addressing major challenges in cardiovascular applications, such as thrombosis, restenosis, and poor endothelialization. The following Table 4 summarizes the design of numerous studies using MOFs as vascular implants in CVDs.

4. Challenges and limitations

Although MOF-based cardiovascular treatments have already been explored successfully with promising results, several limitations remain.

4.1. Structural validation

One major limitation is the need for a deeper understanding of MOF synthesis and structure, which is crucial for advancing the translational potential. Many MOF studies in CVD lack rigorous structural validation, such as PXRD analysis, to confirm that the synthesized MOFs align with the calculated structures. Additionally, even when using the same MOF precursors (such as the MIL series, as shown in Table 2), variations in synthesis conditions like temperature can lead to different MOF structures. PXRD data are essential to verify that the structure corresponds to the intended design, which is essential for advancing MOF-based cardiovascular therapeutics toward clinical application. Furthermore, some ligands, such as epigallocatechin gallate (EGCG) [191,192] and pentagalloyl glucose (PGG) [193] may potentially form MOF structures. However, PXRD analysis is required to confirm whether these ligands truly form crystalline MOF structure. Crystalline MOFs typically display sharp, well-defined peaks at specific 2θ values, corresponding to their characteristic periodic atomic arrangements. The absence of clear peaks may indicate an amorphous coordination polymer or hybrid material rather than a true MOF. Verifying the MOF structure is critical for conducting toxicology and pharmacokinetic studies in vivo, as an unvalidated structure may represent mixtures of MOF precursors or amorphous coordination polymers rather than true MOF structures, potentially introducing toxicity from these components. Furthermore, the absence of clear PXRD peaks typically indicates reduced or absent porosity, significantly impairing drug loading capacities.

Table 4
Summary of MOF-based vascular implants for CVD treatment.

CVDs	MOF	Functional materials	Encapsulated or Loaded materials	Designed structure and concept	Preclinical model	Ref
Stent	Cu-MOF (MOF-199)	Polydopamine film-coated titanium	RSNOs	Cu-MOFs are uniformly distributed as a coating material on the polydopamine-coated titanium substrate (316L SS stents).	Male Sprague-Dawley rats; adult New Zealand white rabbits	[85]
	Cu-MOF	Hydroxylated titanium surface	RSNOs	The hydroxylated titanium foil was alternately immersed in Cu acetate and MOF ligand solutions for multiple cycles using a layer-by-layer deposition process.	Male Sprague-Dawley rats and adult New Zealand white rabbits	[86]
Graft	MOF-199	Polycaprolactone fibers	RSNOs	Vascular scaffolds were electrospun from 10 % (*w/v*) polycaprolactone and MOF nanoparticles.	Sprague-Dawley rats	[87]

Functionalization attempts may also fail to anchor effectively within a structurally undefined material, resulting in poor targeted delivery and reduced therapeutic efficacy. Thus, establishing a structurally validated MOF is essential for consistent and reproducible drug delivery applications. A notable example provided by Serre's group [194] demonstrates that MIL-100(Fe) synthesized using different green methods exhibits subtle differences in PXRD patterns, which in turn are associated with substantial variations in drug release profiles, stability in biological fluids, and distinct in vitro toxicological and inflammatory responses. Consequently, if synthesized materials fail to display distinct PXRD patterns consistent with calculated MOF structures, their reliability for clinical translation and reproducibility is severely compromised. Therefore, rigorous structural validation through PXRD is essential for confirming MOF identity and purity, directly impacting the reliability, reproducibility, and clinical translatability of MOF-based cardiovascular treatments.

4.2. Batch-to-batch reproducibility

MOF synthesis is highly sensitive to various parameters, including solvent composition, temperature, pH, precursor concentrations, and reaction duration. Even minor deviations in these factors can significantly influence critical material properties such as particle size, surface area, porosity, and crystallinity, which directly impact drug loading efficiency, release kinetics, and biological performance. The absence of standardized synthesis and characterization protocols further complicates reproducibility, resulting in notable variability among reportedly identical MOF batches. This variability poses substantial challenges for quality control, limiting the clinical translation of MOFs. For example, the above discussion of variations in the synthesis method of MIL-100 (Fe) has demonstrated significant differences in biological applications [194]. Additionally, a recent cross-laboratory study investigating the synthesis of PCN-222(Zr) revealed substantial reproducibility issues, with only one research group successfully replicating the pure-phase MOF from validated protocols [195]. Likewise, a recent comparative analysis by the Forgan group reviewed ten different publications from 2023 on UiO-66 synthesis intended for biomedical applications [196]. Although these studies used the same synthesis solvent (*N*, *N*-dimethylformamide), the same metal node ($ZrCI_4$), and the same ligand (terephthalic acid), differences in reaction time, modulators, and reaction temperatures resulted in significant structural and functional variations. Those structural differences translated directly into inconsistent drug loading and release behavior. Reported drug loading efficiencies across the ten studies varied widely, ranging from about 10 % up to over 60 %. The studies examined loading with drugs ranging from small molecules, such as 5-fluorouracil [197] and minoxidil [198] to large molecules such as doxorubicin [199]. These findings highlight the importance of matching the MOF's pore size (as shown in Table 2) in relation to the size of the drug or biomolecule to be loaded. If the drug is too large to fit inside the MOF pores, alternative methods, such as one-pot synthesis or biomimetic mineralization, should be considered. Failure to consider pore size may lead to functional site blockage by drugs attached to the surface, potentially resulting in undesirable outcomes.

4.3. Scale-up

The scalability of MOF-based systems for clinical applications presents several inherent challenges that must be explicitly addressed to ensure effective translation from laboratory to clinical settings. As discussed previously, factors such as variations in crystallinity (PXRD) and batch-to-batch reproducibility significantly complicate scale-up efforts. Although some MOFs have already reached industrial commercialization in adsorption applications and can achieve production costs below €20/kg on a ton scale with space-time yields of up to 10,000 kg MOF $m^{-3}{\cdot}d^{-1}$ [200], the clinical-grade synthesis required for therapeutic use introduces additional constraints. The primary constraints include the high cost of ligands, extensive solvent consumption, and limitations of current synthesis methods. Many laboratory-scale MOF syntheses rely on solvothermal or hydrothermal methods characterized by high pressure and long reaction times, which are conditions that are inherently challenging to scale up. Additionally, scaling up reactions can significantly alter MOF nucleation and growth kinetics compared to small-scale syntheses, resulting in inconsistent product quality and reproducibility. To address these challenges, alternative techniques such as microwave and ultrasound irradiation have been developed, enabling rapid and uniform heating that accelerates reaction kinetics [16]. For instance, microwave-assisted hydrothermal synthesis significantly reduces reaction times to just minutes, maintaining high phase purity and yield, making it a promising method for scalable and cost-efficient MOF production. Continuous-flow synthesis methods also offer advantages, such as improved control over nanoparticle size and shape. However, their applicability remains somewhat system-specific, necessitating extensive optimization [171]. Drawing parallels from clinically successful nanoparticles like Doxil liposomes, MOF systems intended for clinical use must comply strictly with Good Manufacturing Practice standards. Compliance involves rigorous protocols for solvent removal, endotoxin clearance, and strict batch-release standards, including structural verification, particle-size distribution control, and comprehensive impurity profiling [53]. Moreover, for MOF-based CVD therapies specifically, identifying suitable MOFs for clinical translation is equally critical, alongside overcoming scaling issues. Over 90,000 MOF structures have been explored, highlighting the structural flexibility of MOFs achieved by selecting different metal nodes and organic ligands. Recently, more targeted functionalization strategies have emerged, further expanding MOF applications. The availability of large-scale synthesis data has enabled researchers to integrate machine learning (ML) and artificial intelligence (AI) into MOF synthesis and functionalization processes [201]. ML algorithms and computational models enable researchers to efficiently predict optimal synthesis pathways and tailor material properties. In the future, as MOFs continue to develop as promising theranostic agents, they can be customized according to disease models and clinical features. ML algorithms will play a crucial role in selecting appropriate metals, ligands, and functionalization strategies to design multifunctional agents tailored to cardiovascular therapeutic needs.

4.4. Biocompatibility and long-term toxicity

Many CVDs require lifelong management, and any treatment, including MOF-based therapies, must be evaluated for its long-term effects on patient health. This raises important concerns about the acute and chronic toxicities of both the MOFs [202] themselves and the drug cargos they carry. While drug-loaded MOFs have the potential to reduce the overall toxicity of harmful drugs by controlling their release and targeting specific sites of action, MOFs, like many nanomaterials, may introduce toxicity due to their composition, structure, or surface properties. To address these concerns, we summarize below the known toxicity profiles of commonly studied MOFs and highlight key mitigation strategies. These include surface functionalization and the use of biomolecular ligands, which have been discussed in detail in Sections 2.2 and 2.4.

Metal-containing nodes: The choice of metal significantly influences the overall toxicity of MOFs [203]. For example, Fe-based MOFs such as MIL-100(Fe) are generally considered biocompatible at low doses, but high concentrations may induce oxidative stress via Fenton chemistry [204]. Zn-based MOFs like ZIF-8 rapidly degrade in acidic environments, releasing Zn ions that can disrupt vascular cell function and elevate CVD risk [205,206]. Co-based MOFs (ZIF-67) are particularly hemolytic due to superoxide anion and ·OH production, resulting in erythrocyte damage [207]. Additionally, non-endogenous metals (Zr, Ni, Co) may accumulate due to poor clearance, with

zirconium-based MOFs such as UiO-66 being associated with potential liver and serum oxidative toxicity [208].

Ligands: Ligands with hydrophobic groups, such as terephthalic acid derivatives bearing methyl or nitro functionalities, exhibit higher toxicity compared to hydrophilic ligands like benzene-1,3,5-tricarboxylic acid, which are readily excreted, reducing their cytotoxic potential [209]. For example, UiO-64 (fumaric acid ligand) is notably more toxic compared to UiO-66 (terephthalic acid ligand), highlighting the ligand's significant role in determining MOF toxicity [210].

Surface charge and particle size: MOFs with positively charged or hydrophobic surfaces are more likely to interact with plasma proteins and cell membranes, raising the risk of inflammation and cytotoxicity. Surface modifications, such as introducing amino groups to ZIF-90, increase its positive charge and cytotoxic effects compared to carboxylated or thiolated analogues [211]. Additionally, particle size plays a crucial role in biomedical safety, with nanoscale MOFs (e.g., 250–350 nm Mg-MOF-74) showing better biocompatibility and promoting tissue growth compared to larger particles [166].

Mitigation strategies: As detailed in Section 2.4, a range of functionalization strategies—including polymer coatings (e.g., PEG, dextran, hyaluronic acid), peptide conjugation, and biomimetic cell membrane coatings—have already been discussed in depth for their roles in enhancing MOF stability, circulation, and biocompatibility [47]. These approaches are also critical for mitigating toxicity. Functionalization reduces inflammatory responses, prevents premature degradation, and facilitates targeted delivery. Cell membrane coatings also present a biomimetic strategy, minimizing immune recognition and improving targeted delivery, thus reducing toxicity [48]. Moreover, employing biomolecular ligands such as amino acids, peptides, or cyclodextrins as described in Section 2.2, is an effective strategy, as they are inherently biodegradable and less toxic, which further mitigates adverse effects [212].

While MOFs hold significant promise for advancing CVD diagnosis and therapy, a comprehensive understanding of their biocompatibility and long-term toxicity within cardiovascular systems remains insufficient. Addressing these gaps through focused toxicological studies and the development of safer, more biodegradable MOF platforms is critical. Such efforts will pave the way for the responsible integration of MOFs into clinical cardiovascular applications, maximizing therapeutic benefits while minimizing potential risks.

5. Conclusion

In this review, we first introduced the basic properties of MOFs and how these properties are applied in the cardiovascular field. We then summarized recent preclinical studies in CVD treatment to explore MOF design principles for achieving therapeutic goals, highlighting their multifunctionality, including drug loading, targeting, and nanozyme capabilities. By bridging the gap between MOF design principles and their preclinical research applications, this review aims to provide a foundational overview for biomedical scientists designing MOF materials from fundamental principles and to assist MOF material scientists in understanding in vivo evaluation and biocompatibility assessment through these preclinical studies and biological evaluations. Furthermore, we identified key challenges and limitations associated with MOF-based cardiovascular treatments, particularly in terms of toxicity, reproducibility, and scalability. Addressing these issues requires standardized protocols for synthesis, surface modification, and biological evaluation to improve consistency and reliability across studies. Overcoming these translational barriers will also demand close interdisciplinary collaboration between material scientists and clinicians to bridge the gap between bench-top innovation and clinical application.

MOFs demonstrate great promise in translational research, as evidenced by the first clinical trial of a MOF-based radioenhancer for solid tumors: RiMO-301 (Phase II: NCT05838729) [65] for metastatic head and neck cancer and RiMO-401 (Phase I: NCT06182579), which started in 2024 for advanced tumors in combination with radiation therapy. Both trials aim to evaluate the safety, tolerability, and preliminary efficacy of MOFs in combination with radiotherapy. Although these studies do not target CVDs, they serve as proof of concept for the clinical viability of MOF-based nanomedicines. The clinical translation of MOFs requires overcoming key challenges, including biocompatibility, biodegradability, toxicity, pharmacokinetics, and manufacturing scalability. Current clinical trials provide valuable insights into addressing these barriers. Although the use of MOFs in CVDs remains limited, promising preclinical data, particularly for applications such as NO delivery, oxidative stress modulation, and anti-inflammatory therapies, underscore their potential for clinical translation [213]. Continued efforts are essential to optimize their design, ensure scalable synthesis, and conduct early-phase safety studies to enable their successful clinical adoption. As more researchers focus on MOF-based cardiovascular therapies, their potential as powerful therapeutic agents for CVDs will continue to grow, offering new hope for treating conditions with high mortality rates.

Declaration of competing interest

The authors declare that they have no known competing financial interests or personal relationships that could have appeared to influence the work reported in this paper.

Acknowledgements

The authors acknowledge the Robert A. Welch Foundation (B-0027 for S.M. and BE0023 for R.I.P.) for the financial support of this work. We also acknowledge funding support from the George and Angelina Kostas Research Center for Cardiovascular Nanomedicine. The authors also extend their appreciation to the Deputyship for Research and Innovation, "Ministry of Education" in Saudi Arabia for funding of this research (IFKSU-HCRA-002-1). We also thank Dr. Raja Muthupillai from Texas A&M University for his insightful revisions and expert guidance on the imaging technology sections of this review article.

Data availability

Data will be made available on request.

References

[1] E.J. Benjamin, M.J. Blaha, S.E. Chiuve, M. Cushman, S.R. Das, R. Deo, S.D. de Ferranti, J. Floyd, M. Fornage, C. Gillespie, C.R. Isasi, M.C. Jimenez, L.C. Jordan, S.E. Judd, D. Lackland, J.H. Lichtman, L. Lisabeth, S. Liu, C.T. Longenecker, R. H. Mackey, K. Matsushita, D. Mozaffarian, M.E. Mussolino, K. Nasir, R. W. Neumar, L. Palaniappan, D.K. Pandey, R.R. Thiagarajan, M.J. Reeves, M. Ritchey, C.J. Rodriguez, G.A. Roth, W.D. Rosamond, C. Sasson, A. Towfighi, C. W. Tsao, M.B. Turner, S.S. Virani, J.H. Voeks, J.Z. Willey, J.T. Wilkins, J.H. Wu, H.M. Alger, S.S. Wong, P. Muntner, C. American Heart Association Statistics, S. Stroke Statistics, Heart Disease and Stroke Statistics-2017 update: a report from the American Heart Association, Circulation 135 (2017) e146–e603.
[2] National Health Service (NHS), Cardiovascular disease. https://www.nhs.uk/conditions/cardiovascular-disease/, 2023 (accessed 20 April 2025).
[3] J.H. Park, D. Dehaini, J. Zhou, M. Holay, R.H. Fang, L. Zhang, Biomimetic nanoparticle technology for cardiovascular disease detection and treatment, Nanoscale Horiz. 5 (2020) 25–42.
[4] R.S. Soumya, K.G. Raghu, Recent advances on nanoparticle-based therapies for cardiovascular diseases, J. Cardiol. 81 (2023) 10–18.
[5] F. Yang, J. Xue, G. Wang, Q. Diao, Nanoparticle-based drug delivery systems for the treatment of cardiovascular diseases, Front. Pharmacol. 13 (2022) 999404.
[6] G.U. Ruiz-Esparza, J.H. Flores-Arredondo, V. Segura-Ibarra, G. Torre-Amione, M. Ferrari, E. Blanco, R.E. Serda, The physiology of cardiovascular disease and innovative liposomal platforms for therapy, Int. J. Nanomed. 8 (2013) 629–640.
[7] L. Li, Y. Zeng, G. Liu, Metal-based nanoparticles for cardiovascular disease diagnosis and therapy, Particuology 72 (2023) 94–111.
[8] J. Della Rocca, D. Liu, W. Lin, Nanoscale metal-organic frameworks for biomedical imaging and drug delivery, Acc. Chem. Res. 44 (10) (2011) 957–968.
[9] N. Yoshinari, T. Konno, Multitopic metal–organic carboxylates available as supramolecular building units, Coord. Chem. Rev. 474 (2023) 214850.

[10] K.O. Kirlikovali, S.L. Hanna, F.A. Son, O.K. Farha, Back to the basics: developing advanced metal-organic frameworks using fundamental chemistry concepts, ACS Nanosci. Au 3 (2023) 37–45.
[11] X. Ge, R. Wong, A. Anisa, S. Ma, Recent development of metal-organic framework nanocomposites for biomedical applications, Biomaterials 281 (2022) 121322.
[12] Nisha Tyagi, Yalini H. Wijesundara, J.J. Gassensmith, A. Popat, Clinical translation of metal–organic frameworks, Nat. Rev. Mater.
[13] M. Lismont, L. Dreesen, S. Wuttke, Metal-organic framework nanoparticles in photodynamic therapy: current status and perspectives, Adv. Funct. Mater. 27 (14) (2017).
[14] K. Lu, T. Aung, N. Guo, R. Weichselbaum, W. Lin, Nanoscale metal-organic frameworks for therapeutic, imaging, and sensing applications, Adv. Mater. 30 (37) (2018) 1707634.
[15] J. Yang, Y.W. Yang, Metal-organic frameworks for biomedical applications, Small 16 (10) (2020) 1906846.
[16] I. Abánades Lázaro, X. Chen, M. Ding, A. Eskandari, D. Fairen-Jimenez, M. Giménez-Marqués, R. Gref, W. Lin, T. Luo, R.S. Forgan, Metal–organic frameworks for biological applications, Nat. Rev. Methods Primers 4 (2024) 42.
[17] K. Lu, C. He, W. Lin, Nanoscale metal-organic framework for highly effective photodynamic therapy of resistant head and neck cancer, J. Am. Chem. Soc. 136 (2014) 16712–16715.
[18] K. Lu, C. He, N. Guo, C. Chan, K. Ni, G. Lan, H. Tang, C. Pelizzari, Y.X. Fu, M. T. Spiotto, R.R. Weichselbaum, W. Lin, Low-dose X-ray radiotherapy-radiodynamic therapy via nanoscale metal-organic frameworks enhances checkpoint blockade immunotherapy, Nat. Biomed. Eng. 2 (2018) 600–610.
[19] H. Wang, Y. Chen, H. Wang, X. Liu, X. Zhou, F. Wang, DNAzyme-loaded metal-organic frameworks (MOFs) for self-sufficient gene therapy, Angew. Chem. Int. Ed. 58 (2019) 7380–7384.
[20] X. Geng, X. Du, W. Wang, C. Zhang, X. Liu, Y. Qu, M. Zhao, W. Li, M. Zhang, K. Tu, Y.Q. Li, Confined cascade metabolic reprogramming nanoreactor for targeted alcohol detoxification and alcoholic liver injury management, ACS Nano 17 (2023) 7443–7455.
[21] P. Horcajada, T. Chalati, C. Serre, B. Gillet, C. Sebrie, T. Baati, J.F. Eubank, D. Heurtaux, P. Clayette, C. Kreuz, J.S. Chang, Y.K. Hwang, V. Marsaud, P. N. Bories, L. Cynober, S. Gil, G. Ferey, P. Couvreur, R. Gref, Porous metal-organic-framework nanoscale carriers as a potential platform for drug delivery and imaging, Nat. Mater. 9 (2010) 172–178.
[22] Phase I Dose-Escalating Study of RiMO-301 With Radiation in Advanced Tumors, ClinicalTrials.gov Identifier: NCT03444714. Available at: https://clinicaltrials.gov/study/NCT03444714 (accessed June 8, 2025).
[23] M.Z. Alyami, S.K. Alsaiari, Y. Li, S.S. Qutub, F.A. Aleisa, R. Sougrat, J. S. Merzaban, N.M. Khashab, Cell-type-specific CRISPR/Cas9 delivery by biomimetic metal organic frameworks, J. Am. Chem. Soc. 142 (2020) 1715–1720.
[24] J. Zhuang, H. Gong, J. Zhou, Q. Zhang, W. Gao, R.H. Fang, L. Zhang, Targeted gene silencing in vivo by platelet membrane–coated metal-organic framework nanoparticles, Sci. Adv. 6 (2020) eaaz6108.
[25] F. Melle, D. Menon, J. Conniot, J. Ostolaza-Paraiso, S. Mercado, J. Oliveira, X. Chen, B.B. Mendes, J. Conde, D. Fairen-Jimenez, Rational design of metal-organic frameworks for pancreatic cancer therapy: from machine learning screening to in vivo efficacy, Adv. Mater. (2025) 2412757.
[26] S.M. Moosavi, A. Nandy, K.M. Jablonka, D. Ongari, J.P. Janet, P.G. Boyd, Y. Lee, B. Smit, H.J. Kulik, Understanding the diversity of the metal-organic framework ecosystem, Nat. Commun. 11 (2020) 4068.
[27] N. Tyagi, Y.H. Wijesundara, J.J. Gassensmith, A. Popat, Clinical translation of metal–organic frameworks, Nat. Rev. Mater. 8 (2023) 701–703.
[28] S. Li, K. Wang, Y. Shi, Y. Cui, B. Chen, B. He, W. Dai, H. Zhang, X. Wang, C. Zhong, H. Wu, Q. Yang, Q. Zhang, Novel biological functions of ZIF-NP as a delivery vehicle: high pulmonary accumulation, Favorable biocompatibility, and improved therapeutic outcome, Adv. Funct. Mater. 26 (2016) 2715–2727.
[29] Y. Zhang, F. Wang, E. Ju, Z. Liu, Z. Chen, J. Ren, X. Qu, Metal-organic-framework-based vaccine platforms for enhanced systemic immune and memory response, Adv. Funct. Mater. 26 (2016) 6454–6461.
[30] J. Xiao, S. Chen, J. Yi, H. Zhang, G.A. Ameer, A cooperative copper metal-organic framework-hydrogel system improves wound healing in diabetes, Adv. Funct. Mater. 27 (2017).
[31] D. Yu, Y. Guan, F. Bai, Z. Du, N. Gao, J. Ren, X. Qu, Metal-organic frameworks harness cu chelating and photooxidation against amyloid beta aggregation in vivo, Chem. A Eur. J. 25 (2019) 3489–3495.
[32] F. Zhang, Y. Liu, J. Lei, S. Wang, X. Ji, H. Liu, Q. Yang, Metal-organic-framework-derived carbon nanostructures for site-specific dual-modality photothermal/photodynamic Thrombus therapy, Adv. Sci. 6 (2019) 1901378.
[33] G.H. Lizhen He, Hongxing Liu, Chengcheng Sang, Xinxin Liu, Tianfeng Chen, Highly bioactive zeolitic imidazolate framework-8-capped nanotherapeutics for efficient reversal of reperfusion-induced injury in ischemic stroke, Sci. Adv. 6 (2020) eaay9751.
[34] W. Duan, S. Qiao, M. Zhuo, J. Sun, M. Guo, F. Xu, J. Liu, T. Wang, X. Guo, Y. Zhang, J. Gao, Y. Huang, Z. Zhang, P. Cheng, S. Ma, Y. Chen, Multifunctional platforms: metal-organic frameworks for cutaneous and cosmetic treatment, Chem 7 (2021) 450–462.
[35] J. Guo, Z. Yang, Y. Lu, C. Du, C. Cao, B. Wang, X. Yue, Z. Zhang, Y. Xu, Z. Qin, T. Huang, W. Wang, W. Jiang, J. Zhang, J. Tang, An antioxidant system through conjugating superoxide dismutase onto metal-organic framework for cardiac repair, Bioact. Mater. 10 (2022) 56–67.
[36] B. Gao, X. Wang, M. Wang, K. You, G.S. Ahmed Suleiman, X.K. Ren, J. Guo, S. Xia, W. Zhang, Y. Feng, Superlow dosage of intrinsically bioactive zinc metal-organic frameworks to modulate endothelial cell morphogenesis and significantly rescue ischemic disease, ACS Nano 16 (2022) 1395–1408.
[37] J. Sheng, Z. Zu, Y. Zhang, H. Zhu, J. Qi, T. Zheng, Y. Tian, L. Zhang, Targeted therapy of atherosclerosis by zeolitic imidazolate framework-8 nanoparticles loaded with losartan potassium via simultaneous lipid-scavenging and anti-inflammation, J. Mater. Chem. B 10 (2022) 5925–5937.
[38] W. Zhang, J. Li, N. Zhao, P. Li, W. Zhang, H. Wang, B. Tang, Ratiometric fluorescence biosensor for imaging of protein phosphorylation levels in atherosclerosis mice, Anal. Chim. Acta 1208 (2022) 339825.
[39] A.P. Acharya, K.B. Sezginel, H.P. Gideon, A.C. Greene, H.D. Lawson, S. Inamdar, Y. Tang, A.J. Fraser, K.V. Patel, C. Liu, N.L. Rosi, S.Y. Chan, J.L. Flynn, C. E. Wilmer, S.R. Little, In silico identification and synthesis of a multi-drug loaded MOF for treating tuberculosis, J. Control. Release 352 (2022) 242–255.
[40] J.-J. Zou, G. Wei, C. Xiong, Y. Yu, S. Li, L. Hu, S. Ma, J. Tian, Efficient oral insulin delivery enabled by transferrin-coated acid-resistant metal-organic framework nanoparticles, Sci. Adv. 8 (2022) eabm4677.
[41] W. Liu, Y. Li, Y. Wang, Y. Feng, Bioactive metal-organic frameworks as a distinctive platform to diagnosis and treat vascular diseases, Small 20 (2024) e2310249.
[42] A. Jenabi, M.A.F. Maghsoudi, M. Daghigh, R. Mehdinavaz Aghdam, Metal organic frameworks for therapeutic approaches in cardiovascular diseases: a comprehensive review, J. Drug Delivery Sci. Technol. 94 (2024) 105489.
[43] R.F. Mendes, F. Figueira, J.P. Leite, L. Gales, F.A. Almeida Paz, Metal-organic frameworks: a future toolbox for biomedicine? Chem. Soc. Rev. 49 (2020) 9121–9153.
[44] H. Cai, Y.-L. Huang, D. Li, Biological metal–organic frameworks: structures, host–guest chemistry and bio-applications, Coord. Chem. Rev. 378 (2019) 207–221.
[45] W. Liang, P. Wied, F. Carraro, C.J. Sumby, B. Nidetzky, C.K. Tsung, P. Falcaro, C. J. Doonan, Metal-organic framework-based enzyme biocomposites, Chem. Rev. 121 (2021) 1077–1129.
[46] L. Ma, F. Jiang, X. Fan, L. Wang, C. He, M. Zhou, S. Li, H. Luo, C. Cheng, L. Qiu, Metal-organic-framework-engineered enzyme-mimetic catalysts, Adv. Mater. 32 (2020) e2003065.
[47] D. Giliopoulos, A. Zamboulis, D. Giannakoudakis, D. Bikiaris, K. Triantafyllidis, Polymer/metal organic framework (MOF) nanocomposites for biomedical applications, Molecules 25 (2020) 185.
[48] W. Liu, Q. Yan, C. Xia, X. Wang, A. Kumar, Y. Wang, Y. Liu, Y. Pan, J. Liu, Recent advances in cell membrane coated metal-organic frameworks (MOFs) for tumor therapy, J. Mater. Chem. B 9 (2021) 4459–4474.
[49] Z. Guo, Y. Xiao, W. Wu, M. Zhe, P. Yu, S. Shakya, Z. Li, F. Xing, Metal-organic framework-based smart stimuli-responsive drug delivery systems for cancer therapy: advances, challenges, and future perspectives, J. Nanobiotechnol. 23 (1) (2025) 157.
[50] S. Pande, Liposomes for drug delivery: review of vesicular composition, factors affecting drug release and drug loading in liposomes, Artif. Cells Nanomed. Biotechnol. 51 (2023) 428–440.
[51] V. Andra, S.V.N. Pammi, L. Bhatraju, L.K. Ruddaraju, A comprehensive review on novel liposomal methodologies, commercial formulations, clinical trials and patents, BioNanoScience 12 (2022) 274–291.
[52] D. Guimaraes, A. Cavaco-Paulo, E. Nogueira, Design of liposomes as drug delivery system for therapeutic applications, Int. J. Pharm. 601 (2021) 120571.
[53] L. Belfiore, D.N. Saunders, M. Ranson, K.J. Thurecht, G. Storm, K.L. Vine, Towards clinical translation of ligand-functionalized liposomes in targeted cancer therapy: challenges and opportunities, J. Control. Release 277 (2018) 1–13.
[54] S.G. Ong, L.C. Ming, K.S. Lee, K.H. Yuen, Influence of the encapsulation efficiency and size of liposome on the Oral bioavailability of griseofulvin-loaded liposomes, Pharmaceutics 8 (2016) 25.
[55] C. Wang, X. Lan, L. Zhu, Y. Wang, X. Gao, J. Li, H. Tian, Z. Liang, W. Xu, Construction strategy of functionalized liposomes and multidimensional application, Small 20 (2024) e2309031.
[56] A. Kumari, S.K. Yadav, S.C. Yadav, Biodegradable polymeric nanoparticles based drug delivery systems, Colloids Surf., B 75 (2010) 1–18.
[57] L.L. Haidar, M. Bilek, B. Akhavan, Surface bio-engineered polymeric nanoparticles, Small 20 (2024) e2310876.
[58] T. Xia, M. Kovochich, M. Liong, H. Meng, S. Kabehie, S. George, J.I. Zink, A. E. Nel, Polyethyleneimine coating enhances the cellular uptake of mesoporous silica nanoparticles and allows safe delivery ofsiRNA and DNA constructs, ACS Nano 3 (2009) 3273–3286.
[59] T.I. Janjua, Y. Cao, F. Kleitz, M. Linden, C. Yu, A. Popat, Silica nanoparticles: a review of their safety and current strategies to overcome biological barriers, Adv. Drug Deliv. Rev. 203 (2023) 115115.
[60] J.L. Slowing II, C.W. Vivero-Escoto, V.S. Wu, Lin, mesoporous silica nanoparticles as controlled release drug delivery and gene transfection carriers, Adv. Drug Deliv. Rev. 60 (2008) 1278–1288.
[61] A.H. Khalbas, T.M. Albayati, N.M.C. Saady, S. Zendehboudi, I.K. Salih, M. L. Tofah, Insights into drug loading techniques with mesoporous silica nanoparticles: optimization of operating conditions and assessment of drug stability, J. Drug Delivery Sci. Technol. 96 (2024) 105489.
[62] R. Zhang, F. Kiessling, T. Lammers, R.M. Pallares, Clinical translation of gold nanoparticles, drug delivery, Transl. Res. 13 (2023) 378–385.
[63] N.G. Khlebtsov, L.A. Dykman, Optical properties and biomedical applications of plasmonic nanoparticles, J. Quant. Spectrosc. Radiat. Transf. 111 (2010) 1–35.
[64] K. Kolouchová, V. Lobaz, H. Beneš, V.R. de la Rosa, D. Babuka, P. Švec, P. Černoch, M. Hrubý, R. Hoogenboom, P. Štěpánek, O. Groborz,

Thermoresponsive properties of polyacrylamides in physiological solutions, Polym. Chem. 12 (35) (2021) 5077–5084.
[65] M. Koshy, M. Spiotto, L.E. Feldman, J.J. Luke, G.F. Fleming, D. Olson, J. W. Moroney, R. Nanda, A. Rosenberg, A.T. Pearson, A. Juloori, F. Weinberg, C. Ray, R.C. Gaba, P.J. Chang, L.A. Janisch, Z.-Q. Xu, W. Lin, R.R. Weichselbaum, S.J. Chmura, A phase 1 dose-escalation study of RiMO-301 with palliative radiation in advanced tumors, J. Clin. Oncol. 41 (2023) 2527.
[66] M.K. Zhang, J.J. Ye, C.X. Li, Y. Xia, Z.Y. Wang, J. Feng, X.Z. Zhang, Cytomembrane-mediated transport of metal ions with biological specificity, Adv. Sci. 6 (2019) 1900835.
[67] H. Bunzen, D. Jirak, Recent advances in metal-organic frameworks for applications in magnetic resonance imaging, ACS Appl. Mater. Interfaces 14 (2022) 50445–50462.
[68] F. Lv, H. Fang, L. Huang, Q. Wang, S. Cao, W. Zhao, Z. Zhou, W. Zhou, X. Wang, Curcumin equipped nanozyme-like metal-organic framework platform for the targeted atherosclerosis treatment with lipid regulation and enhanced magnetic resonance imaging capability, Adv. Sci. 11 (2024) e2309062.
[69] K.E. Dekrafft, W.S. Boyle, L.M. Burk, O.Z. Zhou, W. Lin, Zr- and Hf-based nanoscale metal-organic frameworks as contrast agents for computed tomography, J. Mater. Chem. 22 (2012) 18139–18144.
[70] D. Chen, D. Yang, C.A. Dougherty, W. Lu, H. Wu, X. He, T. Cai, M.E. Van Dort, B. D. Ross, H. Hong, In vivo targeting and positron emission tomography imaging of tumor with intrinsically radioactive metal-organic frameworks nanomaterials, ACS Nano 11 (2017) 4315–4327.
[71] S. Gargiulo, A. Greco, M. Gramanzini, M.P. Petretta, A. Ferro, M. Larobina, M. Panico, A. Brunetti, A. Cuocolo, PET/CT imaging in mouse models of myocardial ischemia, J. Biomed. Biotechnol. 2012 (2012) 541872.
[72] M.M. Meloni, S. Barton, L. Xu, J.C. Kaski, W. Song, T. He, Contrast agents for cardiovascular magnetic resonance imaging: an overview, J. Mater. Chem. B 5 (2017) 5714–5725.
[73] L. Wang, B. Zhu, Y. Deng, T. Li, Q. Tian, Z. Yuan, L. Ma, C. Cheng, Q. Guo, L. Qiu, Biocatalytic and antioxidant nanostructures for ROS scavenging and biotherapeutics, Adv. Funct. Mater. 31 (2021) 2101804.
[74] Z. Xu, L. Chen, Y. Luo, Y.M. Wei, N.Y. Wu, L.F. Luo, Y.B. Wei, J. Huang, Advances in metal-organic framework-based nanozymes in ROS scavenging medicine, Nanotechnology 35 (2024) 362006.
[75] N. Panth, K.R. Paudel, K. Parajuli, Reactive oxygen species: a key hallmark of cardiovascular disease, Adv. Med. 2016 (2016) 9152732.
[76] J. Yan, Y. Zhao, M. Du, C. Cui, Z. Bai, Y. Liu, L. Sun, D. Qin, J. Zhou, X. Wu, B. Li, Stimuli-responsive new horizons for biomedical applications: metal–organic framework-based nanozymes, Small Struct. 5 (2024) 2400029.
[77] D. Wang, D. Jana, Y. Zhao, Metal-organic framework derived nanozymes in biomedicine, Acc. Chem. Res. 53 (2020) 1389–1400.
[78] D. Zhu, Y. Su, Y. Zheng, B. Fu, L. Tang, Y.X. Qin, Zinc regulates vascular endothelial cell activity through zinc-sensing receptor ZnR/GPR39, Am. J. Physiol. Cell Physiol. 314 (2018) C404–C414.
[79] J. Cheng, Y. Dou, J. Li, T. You, Y. Wang, M. Wang, S. Shi, S. Peng, C.-h. Cui, X. Duan, J. Xiao, A thermosensitive hydrogel-copper meta-organic framework composite improves hindlimb ischemia therapy through synergistically enhancing HIF-1α production and inhibiting HIF-1α degradation, Mater. Des. 238 (2024) 112638.
[80] M. Hoop, C.F. Walde, R. Riccò, F. Mushtaq, A. Terzopoulou, X.-Z. Chen, A. J. deMello, C.J. Doonan, P. Falcaro, B.J. Nelson, J. Puigmartí-Luis, S. Pané, Biocompatibility characteristics of the metal organic framework ZIF-8 for therapeutical applications, Appl. Mater. Today 11 (2018) 13–21.
[81] S. Baseeruddin Alvi, M. Mergaye, P.S. Dholaniya, G. Sameer, X. Xu, H. Islam, M. Khan, Metal-organic frameworks as next-generation cardiac therapeutics, Circ. Res. (2024). Abstract We038, American Heart Association Scientific Sessions, pp. AWe038–AWe038.
[82] Y. Zhong, Y. Yang, Y. Xu, B. Qian, S. Huang, Q. Long, Z. Qi, X. He, Y. Zhang, L. Li, W. Hai, X. Wang, Q. Zhao, X. Ye, Design of a Zn-based nanozyme injectable multifunctional hydrogel with ROS scavenging activity for myocardial infarction therapy, Acta Biomater. 177 (2024) 62–76.
[83] J.L. Harding, M.M. Reynolds, Metal organic frameworks as nitric oxide catalysts, J. Am. Chem. Soc. 134 (2012) 3330–3333.
[84] T.A. Tabish, M.J. Crabtree, H.E. Townley, P.G. Winyard, C.A. Lygate, Nitric oxide releasing nanomaterials for cardiovascular applications, JACC: Basic Transl. Sci. 9 (2024) 691–709.
[85] Y. Fan, Y. Zhang, Q. Zhao, Y. Xie, R. Luo, P. Yang, Y. Weng, Immobilization of nano cu-MOFs with polydopamine coating for adaptable gasotransmitter generation and copper ion delivery on cardiovascular stents, Biomaterials 204 (2019) 36–45.
[86] Q. Zhao, Y. Fan, Y. Zhang, J. Liu, W. Li, Y. Weng, Copper-based SURMOFs for nitric oxide generation: hemocompatibility, vascular cell growth, and tissue response, ACS Appl. Mater. Interfaces 11 (2019) 7872–7883.
[87] X. Zhang, Y. Wang, J. Liu, J. Shi, D. Mao, A.C. Midgley, X. Leng, D. Kong, Z. Wang, B. Liu, S. Wang, A metal-organic-framework incorporated vascular graft for sustained nitric oxide generation and long-term vascular patency, Chem. Eng. J. 421 (2021) 129577.
[88] M. Lismont, L. Dreesen, S. Wuttke, Metal-organic framework nanoparticles in photodynamic therapy: current status and perspectives, Adv. Funct. Mater. 27 (2017) 1606314.
[89] K. Xiang, H. Wu, Y. Liu, S. Wang, X. Li, B. Yang, Y. Zhang, L. Ma, G. Lu, L. He, Q. Ni, L. Zhang, MOF-derived bimetallic nanozyme to catalyze ROS scavenging for protection of myocardial injury, Theranostics 13 (2023) 2721–2733.
[90] N. Wen, J. Li, W. Zhang, P. Li, X. Yin, W. Zhang, H. Wang, B. Tang, Monitoring the progression of early atherosclerosis using a fluorescence nanoprobe for the detection and imaging of phosphorylation and glucose levels, Angew. Chem. Int. Ed. 62 (2023) e202302161.
[91] J. Li, N. Zhao, W. Zhang, P. Li, X. Yin, W. Zhang, H. Wang, B. Tang, Assessing the progression of early atherosclerosis mice using a fluorescence Nanosensor for the simultaneous detection and imaging of pH and phosphorylation, Angew. Chem. Int. Ed. 62 (2023) e202215178.
[92] Y. Si, H. Luo, P. Zhang, C. Zhang, J. Li, P. Jiang, W. Yuan, R. Cha, CD-MOFs: from preparation to drug delivery and therapeutic application, Carbohydr. Polym. 323 (2024) 121424.
[93] S.S. Jambhekar, P. Breen, Cyclodextrins in pharmaceutical formulations II: solubilization, binding constant, and complexation efficiency, Drug Discov. Today 21 (2016) 363–368.
[94] C. Yuan, Y. Ye, E. Hu, R. Xie, B. Lu, K. Yu, W. Ding, W. Wang, G. Lan, F. Lu, Thrombotic microenvironment responsive crosslinking cyclodextrin metal-organic framework nanocarriers for precise targeting and thrombolysis, Carbohydr. Polym. 334 (2024) 122058.
[95] R. Ma, X. Chen, T. Hu, F. Huang, X. Li, X. Huang, B. He, L. Feng, J. Kou, B. Yu, Design and therapeutic application of trans-sodium crocetinate-loaded cyclodextrin metal–organic frameworks as an enteric preparation for treating chronic heart failure, Appl. Organomet. Chem. 38 (2024) e7411.
[96] S. Yuan, L. Feng, K. Wang, J. Pang, M. Bosch, C. Lollar, Y. Sun, J. Qin, X. Yang, P. Zhang, Q. Wang, L. Zou, Y. Zhang, L. Zhang, Y. Fang, J. Li, H.C. Zhou, Stable metal-organic frameworks: design, synthesis, and applications, Adv. Mater. 30 (2018) e1704303.
[97] M.X. Wu, Y.W. Yang, Metal-organic framework (MOF)-based drug/cargo delivery and cancer therapy, Adv. Mater. 29 (2017) 1606134.
[98] P. Liu, T. Zhao, K. Cai, P. Chen, F. Liu, D.-J. Tao, Rapid mechanochemical construction of HKUST-1 with enhancing water stability by hybrid ligands assembly strategy for efficient adsorption of SF_6, Chem. Eng. J. 437 (2022) 135364.
[99] H.-Y. Zhang, C. Yang, Q. Geng, H.-L. Fan, B.-J. Wang, M.-M. Wu, Z. Tian, Adsorption of hydrogen sulfide by amine-functionalized metal organic framework (MOF-199): An experimental and simulation study, Appl. Surf. Sci. 497 (2019) 143815.
[100] M.J. Katz, Z.J. Brown, Y.J. Colon, P.W. Siu, K.A. Scheidt, R.Q. Snurr, J.T. Hupp, O.K. Farha, A facile synthesis of UiO-66, UiO-67 and their derivatives, Chem. Commun. 49 (2013) 9449–9451.
[101] S. Jakobsen, D. Gianolio, D.S. Wragg, M.H. Nilsen, H. Emerich, S. Bordiga, C. Lamberti, U. Olsbye, M. Tilset, K.P. Lillerud, Structural determination of a highly stable metal-organic framework with possible application to interim radioactive waste scavenging: Hf-UiO-66, Phys. Rev. B 86 (2012) 125429.
[102] B.T. Yost, B. Gibbons, A. Wilson, A.J. Morris, L.E. McNeil, Vibrational spectroscopy investigation of defects in Zr- and Hf-UiO-66, RSC Adv. 12 (2022) 22440–22447.
[103] X. Ge, J. Mohapatra, E. Silva, G. He, L. Gong, T. Lyu, R.P. Madhogaria, X. Zhao, Y. Cheng, A.M. Al-Enizi, A. Nafady, J. Tian, J.P. Liu, M.H. Phan, F. Taraballi, R. I. Pettigrew, S. Ma, Metal-organic framework as a new type of magnetothermally-triggered on-demand release carrier, Small 20 (2024) e2306940.
[104] M. Lammert, M.T. Wharmby, S. Smolders, B. Bueken, A. Lieb, K.A. Lomachenko, D.D. Vos, N. Stock, Cerium-based metal organic frameworks with UiO-66 architecture: synthesis, properties and redox catalytic activity, Chem. Commun. 51 (2015) 12578–12581.
[105] F.A. Son, A. Atilgan, K.B. Idrees, T. Islamoglu, O.K. Farha, Solvent-assisted linker exchange enabled preparation of cerium-based metal–organic frameworks constructed from redox active linkers, Inorg. Chem. Front. 7 (2020) 984–990.
[106] P. Horcajada, F. Salles, S. Wuttke, T. Devic, D. Heurtaux, G. Maurin, A. Vimont, M. Daturi, O. David, E. Magnier, N. Stock, Y. Filinchuk, D. Popov, C. Riekel, G. Ferey, C. Serre, How linker's modification controls swelling properties of highly flexible iron(III) dicarboxylates MIL-88, J. Am. Chem. Soc. 133 (2011) 17839–17847.
[107] D. Villarroel-Rocha, J. Villarroel-Rocha, S. Amaya-Roncancio, C. Garcia-Carvajal, D.A. Barrera, J. Arroyo-Gomez, D.A. Torres-Ceron, E. Restrepo-Parra, K. Sapag, Influence of pressure and temperature on the flexible behavior of Iron-based MIL-53 with the CO(2) host: a comprehensive experimental and DFT study, ACS Omega 9 (2024) 21930–21938.
[108] K. Guesh, C.A.D. Caiuby, Á. Mayoral, M. Díaz-García, I. Díaz, M. Sanchez-Sanchez, Sustainable preparation of MIL-100(Fe) and its photocatalytic behavior in the degradation of methyl orange in water, Cryst. Growth Des. 17 (2017) 1806–1813.
[109] X. Ge, F. Jiang, M. Wang, M. Chen, Y. Li, J. Phipps, J. Cai, J. Xie, J. Ong, V. Dubovoy, J.G. Masters, L. Pan, S. Ma, Naringin@metal-organic framework as a multifunctional bioplatform, ACS Appl. Mater. Interfaces 15 (2023) 677–683.
[110] J.L. Hui Su, Liansheng Yang, Li Feng, Yongze Liu, Du Ziwen, Liqiu Zhang, Rapid and selective adsorption of a typical aromatic organophosphorus flame retardant on MIL-101-based metal–organic frameworks, RSC Adv. 10 (2020) 2198–2208.
[111] K.S. Park, Z. Ni, A.P. Côté, J.Y. Choi, R. Huang, F.J. Uribe-Romo, H.K. Chae, M. O'Keeffe, O.M. Yaghi, Exceptional chemical and thermal stability of zeolitic imidazolate frameworks, Proc. Natl. Acad. Sci. 103 (2006) 10186–10191.
[112] J. Qiu, X. Xu, B. Liu, Y. Guo, H. Wang, L. Yu, Y. Jiang, C. Huang, B. Fan, Z. Zeng, L. Li, Size-controllable synthesis of ZIF-8and derived nitrogen-rich porous carbon for CO_2 and VOCs adsorption, ChemistrySelect 7 (2022) e202203273.
[113] W. Morris, C.J. Doonan, H. Furukawa, R. Banerjee, O.M. Yaghi, Crystals as molecules: postsynthesis covalent functionalization of zeolitic imidazolate frameworks, J. Am. Chem. Soc. 130 (2008) 12626–12627.

[114] Y. Lei, G. Zhang, Q. Zhang, L. Yu, H. Li, H. Yu, Y. He, Visualization of gaseous iodine adsorption on single zeolitic imidazolate framework-90 particles, Nat. Commun. 12 (2021) 4483.
[115] D. Feng, Z.Y. Gu, J.R. Li, H.L. Jiang, Z. Wei, H.C. Zhou, Zirconium-metalloporphyrin PCN-222: mesoporous metal-organic frameworks with ultrahigh stability as biomimetic catalysts, Angew. Chem. Int. Ed. 51 (2012) 10307–10310.
[116] D. Feng, W.C. Chung, Z. Wei, Z.Y. Gu, H.L. Jiang, Y.P. Chen, D.J. Darensbourg, H. C. Zhou, Construction of ultrastable porphyrin Zr metal-organic frameworks through linker elimination, J. Am. Chem. Soc. 135 (2013) 17105–17110.
[117] N. Huang, S. Yuan, H. Drake, X. Yang, J. Pang, J. Qin, J. Li, Y. Zhang, Q. Wang, D. Jiang, H.C. Zhou, Systematic engineering of single substitution in zirconium metal-organic frameworks toward high-performance catalysis, J. Am. Chem. Soc. 139 (2017) 18590–18597.
[118] D. Shen, G. Wang, Z. Liu, P. Li, K. Cai, C. Cheng, Y. Shi, J.M. Han, C.W. Kung, X. Gong, Q.H. Guo, H. Chen, A.C. Sue, Y.Y. Botros, A. Facchetti, O.K. Farha, T. J. Marks, J.F. Stoddart, Epitaxial growth of gamma-cyclodextrin-containing metal-organic frameworks based on a host-guest strategy, J. Am. Chem. Soc. 140 (2018) 11402–11407.
[119] H. Zheng, Y. Zhang, L. Liu, W. Wan, P. Guo, A.M. Nystrom, X. Zou, One-pot synthesis of metal-organic frameworks with encapsulated target molecules and their applications for controlled drug delivery, J. Am. Chem. Soc. 138 (2016) 962–968.
[120] W. Zhang, J. Xu, P. Li, X. Gao, W. Zhang, H. Wang, B. Tang, Treatment of hyperphosphatemia based on specific interactions between phosphorus and Zr (IV) active centers of nano-MOFs, Chem. Sci. 9 (2018) 7483–7487.
[121] J. Wu, Z. Wang, X. Jin, S. Zhang, T. Li, Y. Zhang, H. Xing, Y. Yu, H. Zhang, X. Gao, H. Wei, Hammett relationship in oxidase-mimicking metal-organic frameworks revealed through a protein-engineering-inspired strategy, Adv. Mater. 33 (2021) e2005024.
[122] W. Liu, Y. Zhang, G. Wei, M. Zhang, T. Li, Q. Liu, Z. Zhou, Y. Du, H. Wei, Integrated cascade nanozymes with antisenescence activities for atherosclerosis therapy, Angew. Chem. Int. Ed. 62 (2023) e202304465.
[123] Y. Liu, M. He, Y. Yuan, C. Nie, K. Wei, T. Zhang, T. Chen, X. Chu, Neutrophil-membrane-coated biomineralized metal-organic framework nanoparticles for atherosclerosis treatment by targeting gene silencing, ACS Nano 17 (2023) 7721–7732.
[124] Z. Xu, Z. Wu, S. Huang, K. Ye, Y. Jiang, J. Liu, J. Liu, X. Lu, B. Li, A metal-organic framework-based immunomodulatory nanoplatform for anti-atherosclerosis treatment, J. Control. Release 354 (2023) 615–625.
[125] C. Zeng, Z. Peng, S. Huang, Z. Xu, Z. Peng, Z. Wu, J. Lei, X. Zhang, J. Qin, K. Ye, B. Li, Z. Zhao, Y. Pan, M. Yin, X. Lu, Metal-organic framework-based nanoplatforms for synergistic anti-atherosclerosis therapy by regulating the PI3K/AKT/MSR1 pathway in macrophages, Nanoscale 17 (2024) 3071–3085.
[126] S. Li, H. Gao, H. Wang, X. Zhao, D. Pan, I. Pacheco-Fernandez, M. Ma, J. Liu, J. Hirvonen, Z. Liu, H.A. Santos, Tailored polysaccharide entrapping metal-organic framework for RNAi therapeutics and diagnostics in atherosclerosis, Bioact. Mater. 43 (2025) 376–391.
[127] Y. Zhang, Y. Liu, T. Zhang, Q. Wang, L. Huang, Z. Zhong, J. Lin, K. Hu, H. Xin, X. Wang, Targeted thrombolytic therapy with metal-organic-framework-derived carbon based platforms with multimodal capabilities, ACS Appl. Mater. Interfaces 13 (2021) 24453–24462.
[128] W. Cao, S. Xie, Y. Liu, P. Ran, Z. Zhang, Q. Fang, X. Li, Shear stress-triggered theranostic nanoparticles for piezoelectric-Fenton-photodynamic thrombolysis and endogenous thrombus imaging, Adv. Funct. Mater. 34 (2023) 2312866.
[129] C.C. Chiang, C.H. Liu, L. Rethi, H.T. Nguyen, A.E. Chuang, Phototactic/photosynthetic/magnetic-powered *Chlamydomonas Reinhardtii*-metal-organic frameworks micro/nanomotors for intelligent thrombolytic management and ischemia alleviation, Adv. Healthc. Mater. 13 (2024) e2401383.
[130] J. Shan, L. Du, X. Wang, S. Zhang, Y. Li, S. Xue, Q. Tang, P. Liu, Ultrasound trigger Ce-based MOF nanoenzyme for efficient thrombolytic therapy, Adv. Sci. 11 (2024) e2304441.
[131] Y. Furukawa, T. Ishiwata, K. Sugikawa, K. Kokado, K. Sada, Nano- and microsized cubic gel particles from cyclodextrin metal-organic frameworks, Angew. Chem. Int. Ed. 51 (2012) 10566–10569.
[132] J. Hao, A. Lv, X. Li, Y. Li, A convergent fabrication of silk fibroin nanoparticles on quercetin loaded metal-organic frameworks for promising nanocarrier of myocardial infraction, Heliyon 9 (2023) e20746.
[133] X. Chen, H. Chen, L. Zhu, M. Zeng, T. Wang, C. Su, G. Vulugundam, P. Gokulnath, G. Li, X. Wang, J. Yao, J. Li, D. Cretoiu, Z. Chen, Y. Bei, Nanoparticle-patch system for localized, effective, and sustained miRNA administration into infarcted myocardium to alleviate myocardial ischemia-reperfusion injury, ACS Nano 18 (2024) 19470–19488.
[134] D. Hu, R. Li, Y. Li, M. Wang, L. Wang, S. Wang, H. Cheng, Q. Zhang, C. Fu, Z. Qian, Q. Wei, Inflammation-targeted nanomedicines alleviate oxidative stress and reprogram macrophages polarization for myocardial infarction treatment, Adv. Sci. 11 (2024) e2308910.
[135] X. Wang, B. Gao, M. Wang, Q. Wang, S. Xia, W. Zhang, X. Meng, Y. Feng, CO delivery nanosystem based on regenerative bioactive zinc MOFs highlights intercellular crosstalk for enhanced vascular remodeling in CLI therapy, Chem. Eng. J. 452 (2023) 139670.
[136] X. Wang, B. Gao, S. Xia, W. Zhang, X. Chen, Z. Li, X. Meng, Y. Feng, Surface-functionalized zinc MOFs delivering zinc ion and hydrogen sulfide as tailored anti-hindlimb ischemic nanomedicine, Appl. Mater. Today 32 (2023) 101843.
[137] J. Hu, Z. Xu, D. Liao, Y. Jiang, H. Pu, Z. Wu, X. Xu, Z. Zhao, J. Liu, X. Lu, X. Liu, B. Li, An H_2S-BMP6 dual-loading system with regulating yap/Taz and Jun pathway for synergistic critical limb ischemia salvaging therapy, Adv. Healthc. Mater. 12 (2023) e2301316.
[138] P.J. Jodlowski, G. Kurowski, L. Kuterasinski, M. Sitarz, P. Jelen, J. Jaskowska, A. Kolodziej, A. Pajdak, Z. Majka, A. Boguszewska-Czubara, Cracking the chloroquine conundrum: the application of defective UiO-66 metal-organic framework materials to prevent the onset of heart defects-in vivo and in vitro, ACS Appl. Mater. Interfaces 13 (2021) 312–323.
[139] Y.H. Hong, M. Narwane, L.Y. Liu, Y.D. Huang, C.W. Chung, Y.H. Chen, B.W. Liao, Y.H. Chang, C.R. Wu, H.C. Huang, I.J. Hsu, L.Y. Cheng, L.Y. Wu, Y.L. Chueh, Y. Chen, C.H. Lin, T.T. Lu, Enhanced Oral NO delivery through bioinorganic engineering of acid-sensitive prodrug into a transformer-like DNIC@MOF microrod, ACS Appl. Mater. Interfaces 14 (2022) 3849–3863.
[140] J. Lei, X. Dong, Y. Huang, Z. Wu, Z. Peng, B. Li, R. Wang, Y. Pan, X. Zheng, Z. Zhao, X. Lu, Enhanced vascular smooth muscle cell and extracellular matrix repair using a metal-organic framework-based co-delivery system for abdominal aortic aneurysm therapy, Adv. Healthc. Mater. 14 (2025) e2402937.
[141] C. Doonan, R. Ricco, K. Liang, D. Bradshaw, P. Falcaro, Metal-organic frameworks at the biointerface: synthetic strategies and applications, Acc. Chem. Res. 50 (2017) 1423–1432.
[142] M. Maeki, S. Uno, A. Niwa, Y. Okada, M. Tokeshi, Microfluidic technologies and devices for lipid nanoparticle-based RNA delivery, J. Control. Release 344 (2022) 80–96.
[143] G.-Y. Jeong, R. Ricco, K. Liang, J. Ludwig, J.-O. Kim, P. Falcaro, D.-P. Kim, Bioactive MIL-88A framework hollow spheres via interfacial reaction in-droplet microfluidics for enzyme and nanoparticle encapsulation, Chem. Mater. 27 (2015) 7903–7909.
[144] Y. Wang, C. Hou, Y. Zhang, F. He, M. Liu, X. Li, Preparation of graphene nano-sheet bonded PDA/MOF microcapsules with immobilized glucose oxidase as a mimetic multi-enzyme system for electrochemical sensing of glucose, J. Mater. Chem. B 4 (2016) 3695–3702.
[145] Y. He, D. Li, L. Wu, X. Yin, X. Zhang, L.H. Patterson, J. Zhang, Metal-organic frameworks for gene therapy and detection, Adv. Funct. Mater. 33 (2023) 2212277.
[146] K. Liang, R. Ricco, C.M. Doherty, M.J. Styles, S. Bell, N. Kirby, S. Mudie, D. Haylock, A.J. Hill, C.J. Doonan, P. Falcaro, Biomimetic mineralization of metal-organic frameworks as protective coatings for biomacromolecules, Nat. Commun. 6 (2015) 7240.
[147] Y.V. Kaneti, S. Dutta, M.S.A. Hossain, M.J.A. Shiddiky, K.-L. Tung, F.-K. Shieh, C.-K. Tsung, K.C.-W. Wu, Y. Yamauchi, Strategies for improving the functionality of zeolitic imidazolate frameworks: tailoring nanoarchitectures for functional applications, Adv. Mater. 29 (38) (2017) 1700213.
[148] Q. Yang, Q. Xu, H.L. Jiang, Metal-organic frameworks meet metal nanoparticles: synergistic effect for enhanced catalysis, Chem. Soc. Rev. 46 (2017) 4774–4808.
[149] Y. Liu, D. Yu, X. Ge, L. Huang, P.-Y. Pan, H. Shen, R.I. Pettigrew, S.-H. Chen, J. Mai, Novel platinum therapeutics induce rapid cancer cell death through triggering intracellular ROS storm, Biomaterials 314 (2025) 122835.
[150] S.A. Dabravolski, V.N. Sukhorukov, A.A. Melnichenko, V.A. Khotina, A. N. Orekhov, The role of selenium in atherosclerosis development, progression, prevention and treatment, Biomedicines 11 (2023) 2010.
[151] J. Della Rocca, D. Liu, W. Lin, Nanoscale metal–organic frameworks for biomedical imaging and drug delivery, Acc. Chem. Res. 44 (2011) 957–968.
[152] K.K. Tanabe, S.M. Cohen, Postsynthetic modification of metal–organic frameworks—a progress report, Chem. Soc. Rev. 40 (2011) 498–519.
[153] I. Abanades Lazaro, S. Haddad, S. Sacca, C. Orellana-Tavra, D. Fairen-Jimenez, R. S. Forgan, Selective surface PEGylation of UiO-66 nanoparticles for enhanced stability, cell uptake, and pH-responsive drug delivery, Chem 2 (2017) 561–578.
[154] M. Gimenez-Marques, E. Bellido, T. Berthelot, T. Simon-Yarza, T. Hidalgo, R. Simon-Vazquez, A. Gonzalez-Fernandez, J. Avila, M.C. Asensio, R. Gref, P. Couvreur, C. Serre, P. Horcajada, GraftFast surface engineering to improve MOF nanoparticles furtiveness, Small 14 (2018) e1801900.
[155] X. Chen, Y. Zhuang, N. Rampal, R. Hewitt, G. Divitini, C.A. O'Keefe, X. Liu, D. J. Whitaker, J.W. Wills, R. Jugdaohsingh, J.J. Powell, H. Yu, C.P. Grey, O. A. Scherman, D. Fairen-Jimenez, Formulation of metal-organic framework-based drug carriers by controlled coordination of methoxy PEG phosphate: boosting colloidal stability and Redispersibility, J. Am. Chem. Soc. 143 (2021) 13557–13572.
[156] J. Shen, M. Ma, H. Zhang, H. Yu, F. Xue, N. Hao, H. Chen, Microfluidics-assisted surface trifunctionalization of a zeolitic imidazolate framework nanocarrier for targeted and controllable multitherapies of tumors, ACS Appl. Mater. Interfaces 12 (2020) 45838–45849.
[157] G. Cutrone, J. Qiu, M. Menendez-Miranda, J.M. Casas-Solvas, A. Aykac, X. Li, D. Foulkes, B. Moreira-Alvarez, J.R. Encinar, C. Ladaviere, D. Desmaele, A. Vargas-Berenguel, R. Gref, Comb-like dextran copolymers: a versatile strategy to coat highly porous MOF nanoparticles with a PEG shell, Carbohydr. Polym. 223 (2019) 115085.
[158] R.G. Pearson, Hard and soft acids and bases, J. Am. Chem. Soc. 85 (1963) 3533–3539.
[159] R. Gref, M. Lück, P. Quellec, M. Marchand, E. Dellacherie, S. Harnisch, T. Blunk, R.H. Müller, 'Stealth' corona-core nanoparticles surface modified by polyethylene glycol (PEG): influences of the corona (PEG chain length and surface density) and of the core composition on phagocytic uptake and plasma protein adsorption, Colloids Surf., B 18 (2000) 301–313.
[160] F.A. Jaffer, P. Libby, R. Weissleder, Molecular and cellular imaging of atherosclerosis: emerging applications, J. Am. Coll. Cardiol. 47 (2006) 1328–1338.

[161] H. Zhang, Q. Li, R. Liu, X. Zhang, Z. Li, Y. Luan, A versatile prodrug strategy to in situ encapsulate drugs in MOF nanocarriers: a case of cytarabine-IR820 prodrug encapsulated ZIF-8 toward chemo-photothermal therapy, Adv. Funct. Mater. 28 (2018) 1802830.
[162] Z. Cao, G. Yuan, L. Zeng, L. Bai, X. Liu, M. Wu, R. Sun, Z. Chen, Y. Jiang, Q. Gao, Y. Chen, Y. Zhang, Y. Pan, J. Wang, Macrophage-targeted sonodynamic/photothermal synergistic therapy for preventing atherosclerotic plaque progression using CuS/TiO_2 heterostructured nanosheets, ACS Nano 16 (2022) 10608–10622.
[163] S. Marqus, E. Pirogova, T.J. Piva, Evaluation of the use of therapeutic peptides for cancer treatment, J. Biomed. Sci. 24 (2017) 21.
[164] S. Rojas, T. Devic, P. Horcajada, Metal organic frameworks based on bioactive components, J. Mater. Chem. B 5 (2017) 2560–2573.
[165] H. Zhao, L. Gong, H. Wu, C. Liu, Y. Liu, C. Xiao, C. Liu, L. Chen, M. Jin, Z. Gao, Y. Guan, W. Huang, Development of novel paclitaxel-loaded ZIF-8 metal-organic framework nanoparticles modified with peptide dimers and an evaluation of its inhibitory effect against prostate cancer cells, Pharmaceutics 15 (2023) 1874.
[166] Z. Zhu, S. Jiang, Y. Liu, X. Gao, S. Hu, X. Zhang, C. Huang, Q. Wan, J. Wang, X. Pei, Micro or nano: evaluation of biosafety and biopotency of magnesium metal organic framework-74 with different particle sizes, Nano Res. 13 (2020) 511–526.
[167] Y. Chen, R. Lyu, J. Wang, Q. Cheng, Y. Yu, S. Yang, C. Mao, M. Yang, Metal-organic frameworks nucleated by silk fibroin and modified with tumor-targeting peptides for targeted multimodal cancer therapy, Adv. Sci. 10 (2023) e2302700.
[168] Y. Ma, Y. Ma, M. Gao, Z. Han, W. Jiang, Y. Gu, Y. Liu, Platelet-mimicking therapeutic system for noninvasive mitigation of the progression of atherosclerotic plaques, Adv. Sci. 8 (2021) 2004128.
[169] X. Wei, M. Ying, D. Dehaini, Y. Su, A.V. Kroll, J. Zhou, W. Gao, R.H. Fang, S. Chien, L. Zhang, Nanoparticle functionalization with platelet membrane enables multifactored biological targeting and detection of atherosclerosis, ACS Nano 12 (2018) 109–116.
[170] N. Zheng, K. Li, L. He, Q. Wang, B. Yang, C. Mao, W. Tang, S. Liu, S. Liu, Metal-organic frameworks derived emerging theranostic platforms, Nano Today 58 (2024) 102404.
[171] Y. Sun, B. Xu, X. Pan, H. Wang, Q. Wu, S. Li, B. Jiang, H. Liu, Carbon-based nanozymes: design, catalytic mechanism, and bioapplication, Coord. Chem. Rev. 475 (2023) 214896.
[172] C.L. Galindo, S. Khan, X. Zhang, Y.S. Yeh, Z. Liu, B. Razani, Lipid-laden foam cells in the pathology of atherosclerosis: shedding light on new therapeutic targets, Expert Opin. Ther. Targets 27 (2023) 1231–1245.
[173] Y. Gui, H. Zheng, R.Y. Cao, Foam cells in atherosclerosis: novel insights into its origins, consequences, and molecular mechanisms, Front. Cardiovasc. Med. 9 (2022) 845942.
[174] W.N. Nowak, J. Deng, X.Z. Ruan, Q. Xu, Reactive oxygen species generation and atherosclerosis, Arterioscler. Thromb. Vasc. Biol. 37 (2017) e41–e52.
[175] M. Ouimet, V. Franklin, E. Mak, X. Liao, I. Tabas, Y.L. Marcel, Autophagy regulates cholesterol efflux from macrophage foam cells via lysosomal acid lipase, Cell Metab. 13 (2011) 655–667.
[176] X. Liao, J.C. Sluimer, Y. Wang, M. Subramanian, K. Brown, J.S. Pattison, J. Robbins, J. Martinez, I. Tabas, Macrophage autophagy plays a protective role in advanced atherosclerosis, Cell Metab. 15 (2012) 545–553.
[177] P. Duewell, H. Kono, K.J. Rayner, C.M. Sirois, G. Vladimer, F.G. Bauernfeind, G. S. Abela, L. Franchi, G. Nunez, M. Schnurr, T. Espevik, E. Lien, K.A. Fitzgerald, K. L. Rock, K.J. Moore, S.D. Wright, V. Hornung, E. Latz, NLRP3 inflammasomes are required for atherogenesis and activated by cholesterol crystals, Nature 464 (2010) 1357–1361.
[178] P. Libby, The changing nature of atherosclerosis: what we thought we knew, what we think we know, and what we have to learn, Eur. Heart J. 42 (2021) 4781–4782.
[179] A.M. Morrison, A.E. Sullivan, A.W. Aday, Atherosclerotic disease: pathogenesis and approaches to management, Med. Clin. North Am. 107 (2023) 793–805.
[180] X. Pan, L. Bai, H. Wang, Q. Wu, H. Wang, S. Liu, B. Xu, X. Shi, H. Liu, Metal-organic-framework-derived carbon nanostructure augmented sonodynamic cancer therapy, Adv. Mater. 30 (2018) e1800180.
[181] K. Thygesen, J.S. Alpert, A.S. Jaffe, B.R. Chaitman, J.J. Bax, D.A. Morrow, H.D. White, Fourth universal definition of myocardial infarction (2018), Eur. Heart J. 40 (2019) 237–269.
[182] R. Hofmann, S.K. James, T. Jernberg, B. Lindahl, D. Erlinge, N. Witt, G. Arefalk, M. Frick, J. Alfredsson, L. Nilsson, A. Ravn-Fischer, E. Omerovic, T. Kellerth, D. Sparv, U. Ekelund, R. Linder, M. Ekstrom, J. Lauermann, U. Haaga, J. Pernow, O. Ostlund, J. Herlitz, L. Svensson, Oxygen therapy in suspected acute myocardial infarction, N. Engl. J. Med. 377 (2017) 1240–1249.
[183] H. Bugger, K. Pfeil, Mitochondrial ROS in myocardial ischemia reperfusion and remodeling, Biochim. Biophys. Acta Mol. basis Dis. 1866 (2020) 165768.
[184] X. Wang, B. Su, B. Gao, J. Zhou, X.K. Ren, J. Guo, S. Xia, W. Zhang, Y. Feng, Cascaded bio-responsive delivery of eNOS gene and ZNF(580) gene to collaboratively treat hindlimb ischemia via pro-angiogenesis and anti-inflammation, Biomater. Sci. 8 (2020) 6545–6560.
[185] X. Wang, B. Gao, G. Sebit Ahmed Suleiman, X.-K. Ren, J. Guo, S. Xia, W. Zhang, Y. Feng, A "controlled CO release" and "pro-angiogenic gene" dually engineered stimulus-responsive nanoplatform for collaborative ischemia therapy, Chem. Eng. J. 424 (2021) 129577.
[186] C. Li, O. Kitzerow, F. Nie, J. Dai, X. Liu, M.A. Carlson, G.P. Casale, I.I. Pipinos, X. Li, Bioengineering strategies for the treatment of peripheral arterial disease, Bioact. Mater. 6 (2021) 684–696.
[187] J. Duan, Z. Chen, X. Liang, Y. Chen, H. Li, X. Tian, M. Zhang, X. Wang, H. Sun, D. Kong, Y. Li, J. Yang, Construction and application of therapeutic metal-polyphenol capsule for peripheral artery disease, Biomaterials 255 (2020) 120199.
[188] I.S. Park, C. Mahapatra, J.S. Park, K. Dashnyam, J.W. Kim, J.C. Ahn, P.S. Chung, D.S. Yoon, N. Mandakhbayar, R.K. Singh, J.H. Lee, K.W. Leong, H.W. Kim, Revascularization and limb salvage following critical limb ischemia by nanoceria-induced Ref-1/APE1-dependent angiogenesis, Biomaterials 242 (2020) 119919.
[189] Z. Qi, W. Shi, Y. Zhao, X. Ji, K.J. Liu, Zinc accumulation in mitochondria promotes ischemia-induced BBB disruption through Drp1-dependent mitochondria fission, Toxicol. Appl. Pharmacol. 377 (2019) 114601.
[190] J.S. Isenberg, L.A. Ridnour, E.M. Perruccio, M.G. Espey, D.A. Wink, D.D. Roberts, Thrombospondin-1 inhibits endothelial cell responses to nitric oxide in a cGMP-dependent manner, Proc. Natl. Acad. Sci. 102 (2005) 13141–13146.
[191] C. Tang, H. Wang, L. Guo, Y. Cui, C. Zou, J. Hu, H. Zhang, G. Yang, W. Zhou, Multifunctional nanomedicine for targeted atherosclerosis therapy: activating plaque clearance cascade and suppressing inflammation, ACS Nano 19 (2025) 3339–3361.
[192] A. Zhang, K. Liu, X. Liang, H. Li, X. Fu, N. Zhu, F. Li, J. Yang, Metal-phenolic capsules with ROS scavenging reshape the oxidative microenvironment of atherosclerosis, Nanomed.: Nanotechnol. Biol. Med. 53 (2023) 102700.
[193] H.L. Zu, P.P. Zhuang, Y. Peng, C. Peng, C. Peng, Z.J. Zhu, Y. Yao, J. Yue, Q. S. Wang, W.H. Zhou, H.Y. Wang, Dual-drug nanomedicine assembly with synergistic anti-aneurysmal effects via inflammation suppression and extracellular matrix stabilization, Small 20 (2024) e2402141.
[194] X. Ma, Z. Yu, F. Nouar, I. Dovgaliuk, G. Patriarche, N. Sadovnik, M. Daturi, J.-M. Grenèche, M. Lepoitevin, C. Serre, How defects impact the in vitro behavior of Iron carboxylate MOF nanoparticles, Chem. Mater. 36 (2023) 167–182.
[195] H.L.B. Bostrom, S. Emmerling, F. Heck, C. Koschnick, A.J. Jones, M.J. Cliffe, R. Al Natour, M. Bonneau, V. Guillerm, O. Shekhah, M. Eddaoudi, J. Lopez-Cabrelles, S. Furukawa, M. Romero-Angel, C. Marti-Gastaldo, M. Yan, A.J. Morris, I. Romero-Muniz, Y. Xiong, A.E. Platero-Prats, J. Roth, W.L. Queen, K.S. Mertin, D.E. Schier, N.R. Champness, H.H. Yeung, B.V. Lotsch, How reproducible is the synthesis of Zr-porphyrin metal-organic frameworks? An interlaboratory study, Adv. Mater. 36 (2024) e2304832.
[196] R.S. Forgan, Reproducibility in research into metal-organic frameworks in nanomedicine, Commun. Mater. 5 (2024) 46.
[197] Y. Li, J. Zhao, Y. Wang, T. Zhao, Y. Song, F. Liang, PEGylated chitosan decorated UiO-66 nanoscale metal–organic frameworks as promising carriers for drug delivery, Colloid Polym. Sci. 301 (2023) 1475–1486.
[198] T. Zhang, B. Sun, W. Ding, C. Zhang, X. Yin, B. Wang, J. Ren, Combining rapid degrading microneedles with slow-released drug delivery system for the treatment of alopecia areata, Chem. Eng. J. 471 (2023) 144351.
[199] C. Carrillo-Carrion, V. Comaills, A.M. Visiga, B.R. Gauthier, N. Khiar, Enzyme-responsive Zr-based metal-organic frameworks for controlled drug delivery: taking advantage of clickable PEG-phosphate ligands, ACS Appl. Mater. Interfaces 15 (2023) 27600–27611.
[200] Z. Chen, M.C. Wasson, R.J. Drout, L. Robison, K.B. Idrees, J.G. Knapp, F.A. Son, X. Zhang, W. Hierse, C. Kuhn, S. Marx, B. Hernandez, O.K. Farha, The state of the field: from inception to commercialization of metal-organic frameworks, Faraday Discuss. 225 (2021) 9–69.
[201] Z. Han, Y. Yang, J. Rushlow, J. Huo, Z. Liu, Y.C. Hsu, R. Yin, M. Wang, R. Liang, K. Y. Wang, H.C. Zhou, Development of the design and synthesis of metal-organic frameworks (MOFs)-from large scale attempts, functional oriented modifications, to artificial intelligence (AI) predictions, Chem. Soc. Rev. 54 (2025) 367–395.
[202] L. Yang, H. Chen, A.E. Kaziem, X. Miao, S. Huang, D. Cheng, H. Xu, Z. Zhang, Effects of exposure to different types of metal-organic framework nanoparticles on the gut microbiota and liver metabolism of adult zebrafish, ACS Nano 18 (2024) 25425–25445.
[203] P. Wiśniewska, J. Haponiuk, M.R. Saeb, N. Rabiee, S.A. Bencherif, Mitigating metal-organic framework (MOF) toxicity for biomedical applications, Chem. Eng. J. 471 (2023) 144400.
[204] R. Grall, T. Hidalgo, J. Delic, A. Garcia-Marquez, S. Chevillard, P. Horcajada, In vitro biocompatibility of mesoporous metal (III; Fe, Al, Cr) trimesate MOF nanocarriers, J. Mater. Chem. B 3 (2015) 8279–8292.
[205] Z. Chen, J. Duan, Y. Diao, Y. Chen, X. Liang, H. Li, Y. Miao, Q. Gao, L. Gui, X. Wang, J. Yang, Y. Li, ROS-responsive capsules engineered from EGCG-zinc networks improve therapeutic angiogenesis in mouse limb ischemia, Bioact. Mater. 6 (2021) 1–11.
[206] D. Kota, L. Kang, A. Rickel, J. Liu, S. Smith, Z. Hong, C. Wang, Low doses of zeolitic imidazolate framework-8 nanoparticles alter the actin organization and contractility of vascular smooth muscle cells, J. Hazard. Mater. 414 (2021) 125514.
[207] F. Hao, X.P. Yan, Nano-sized zeolite-like metal-organic frameworks induced hematological effects on red blood cell, J. Hazard. Mater. 424 (2022) 127353.
[208] Y. Yang, H. Bao, Q. Chai, Z. Wang, Z. Sun, C. Fu, Z. Liu, Z. Liu, X. Meng, T. Liu, Toxicity, biodistribution and oxidative damage caused by zirconia nanoparticles after intravenous injection, Int. J. Nanomedicine 14 (2019) 5175–5186.
[209] C. Tamames-Tabar, D. Cunha, E. Imbuluzqueta, F. Ragon, C. Serre, M.J. Blanco-Prieto, P. Horcajada, Cytotoxicity of nanoscaled metal-organic frameworks, J. Mater. Chem. B 2 (2014) 262–271.
[210] I. Sifaoui, I. Pacheco-Fernandez, J.E. Pinero, V. Pino, J. Lorenzo-Morales, A simple in vivo assay using amphipods for the evaluation of potential biocompatible metal-organic frameworks, Front. Bioeng. Biotechnol. 9 (2021) 584115.
[211] C.I. Yen, S.M. Liu, W.S. Lo, J.W. Wu, Y.H. Liu, R.J. Chein, R. Yang, K.C. Wu, J. R. Hwu, N. Ma, F.K. Shieh, Cytotoxicity of postmodified zeolitic imidazolate

Framework-90 (ZIF-90) nanocrystals: correlation between functionality and toxicity, Chem. A Eur. J. 22 (2016) 2925–2929.
[212] I. Imaz, M. Rubio-Martinez, J. An, I. Sole-Font, N.L. Rosi, D. Maspoch, Metal-biomolecule frameworks (MBioFs), Chem. Commun. 47 (2011) 7287–7302.
[213] Q. Wu, Y. Feng, M. Lepoitevin, M. Yu, C. Serre, J. Ge, Y. Huang, Metal-organic frameworks: unlocking new Frontiers in cardiovascular diagnosis and therapy, Adv. Sci. 12 (2025) 2416302.